DEVELOPMENT OF VISIBLE LIGHT-ACTIVE CATALYSTS FOR MTBE REMOVAL FROM GROUND WATER

BY

SALEH HAMAD AL-SHARIDI

A Thesis Presented to the

DEANSHIP OF GRADUATE STUDIES

KING FAHD UNIVERSITY OF PETROLEUM & MINERALS

DHAHRAN, SAUDI ARABIA

In Partial Fulfillment of the
Requirements for the Degree of

MASTER OF SCIENCE

In

CHEMISTRY

June 2013

KING FAHD UNIVERSITY OF PETROLEUM & MINERALS
DHAHRAN, SAUDI ARABIA
DEANSHIP OF GRADATES STUDIES

This thesis, written by Saleh Hamad Al-Sharidi under the direction of his advisor and approved by his thesis committee, has been presented to and accepted the Dean of Graduate Studies, in partial fulfillment of the requirements for the degree of MASTER OF SCIENCE in CHEMISTRY

Thesis Committee

Dr. Khalid R. Alhooshani

Dr. Mohammad Qamar

Dr. Abdel-Nasser M. Kawde

Dr. Basheer Chanbasha

Dr. Abdulaziz A. Alsaadi

for Dr. Abdullah J. Al-Hamdan
Chemistry Department Chairman

Dr. Salam A. Zummo
Dean of Graduate Studies

Date: 26/6/13

This thesis is dedicated

To:

This journey would not have been possible without the support of my family: My beloved mother for her prayers and my wife and daughters for taking their joy time.

ACKNOWLEDGEMENT

I acknowledge King Fahd University of Petroleum and Minerals (KFUPM) for giving me the opportunity to pursue my master's degree by part time study.

I wish to express my appreciation to my committee advisor Dr. Khalid Alhooshani for his support and directions as well as the other committee members: Dr. Mohammad Qamar, Dr. Abdel-Nasser Kawde, Dr. Basheer Chanbasha and Dr. Abdulaziz Alsaadi.

Iam grateful to the chemistry department chairman Dr. Abdullah Al-Hamdan and my advisor Dr. Bassam Al-Ali for their assistance and help during my studies.

Thanks to Saudi Aramco management and special thanks is to: Ali Al-Suliman, Emad Al-Shafei, Ammar Al-Ahmed, Dr. Hameed Al-Badiary, Dr. Husinayah Sitepu and Nasser Bin Hoban.

TABLE OF CONTENT

LIST OF FIGURES

LIST OF TABLES

THESIS ABSTRACT

NAME: SALEH HAMAD AL-SHARIDI

TITLE: DEVELOPMENT OF VISIBLE LIGHT-ACTIVE CATALYSTS FOR MTBE REMOVAL FROM GROUND WATER

MAJOR: CHEMISTRY

DATE: MAY 2013

Tungsten oxide (WO_3) was used as visible-light active photocatalyst for the removal of methyl tertiary butyl ether (MTBE) from contaminated groundwater. Visible-light-driven WO_3 nanostructured photocatalyst was synthesized using a hydrothermal method. For comparison of photocatalytic activity, commercial micron-sized tungsten oxide was also used. The surface of photocatalysts was further modified with noble metals such as platinum (Pt) and ruthenium (Ru) and resulting activity of samples were compared. The experimental results indicated that the removal of MTBE could be achieved very fast in presence of Pt-loaded nanostructured WO_3 under visible light radiation (96-99% removal within 150-180 minutes). The Pt/WO_3 nano-composite showed much better photocatalytic removal of MTBE than Ru/WO_3 and pure nanostructured and micron-sized WO_3. An attempt was also made to study the formation of by-products during photocatalytic degradation of MTBE using GC-MS. The study revealed that the degradation of MTBE proceeds essentially via formation of formic acid and 1, 1-dimethylethyl ester before its complete degradation.

THESIS (ARABIC)

ملخص الرسالة

الاسم: صالح حمد الشريدي

العنوان: تطوير المواد الحفازة الضوئية لمعالجة ميثيل ثالثي بوتيل الإيثرمن المياه الجوفية

الدرجة: ماجستير

التخصص: كيمياء

التاريخ: مايو ٢٠١٣

التنغستن المؤكسد نشط في الاشعة الضوئية وتم اختبارة كمادة محفزه لمعالجة ميثيل ثالثي بوتيل الإيثر(MTBE) من المياه الجوفية . تم تصنيعه نانومتري للتنغستن المؤكسد تحت تسليط الاشعة الضوئية ومن ثم تجهيزه تحت الحرارة المائية. وكذلك تم مقارنة النشاط الضوئي للنانومتري للتنغستن المؤكسد مع التنغستن الموكسد التجاري. وتم تطوير ومقارنة سطح الحافاز الضوئي بأضافة معادن اخرى من البلاتين و الروثينيوم.

النتائج المخبرية توصلت المعالجة السريع لميثيل ثالثي بوتيل الإيثر حوالي ٩٦ – ٩٩% باستخدام الضوئي للنانومتري للتنغستن المؤكسد المضاف اليه عنصر البلاتين تحت الاشعه الضوئية بين ١٥٠ – ١٨٠ دقيقة من المعالجة . وكذلك اظهرت النتائج البلاتين المضاف الى للنانومتري للتنغستن المؤكسد افضل في المعالجة مقارنة مع الروثينيوم المضاف الى للتنغستن المؤكسد والتجاري. وبواسطة الكروماتوغرافيا الغاز بالمطياف الكتلة تم معرفة ١- ١،ثنائي ميثل استر حمض الفورميك المنتج المصاحب اثناء معالجة لميثيل ثالثي بوتيل الإيثر من الماء.

NOMENCLATURE

BTEX	Benzene, toluene, ethylbenzene, and xylenes
CO_2	Carbon dioxide
DW	Distilled water
EDS	Energy Dispersive X-ray Spectroscopy system
EPA	Environmental Protection Agency
ESEM	Environmental Scanning Electron Microcopy
GC-MS	Gas chromatography mass spectrometry
H_2O_2	Hydrogen peroxide
MCL	Maximum Contaminant Level
Mg/L	Milligram per liter
MTBE	Methyl-Tert-Butyl Ether
nm	Nano meter
O_3	Ozone
Oxyfuel	Oxygenated fuel
ppb	Parts per billion
ppm	Parts per million
RSD	Relative standard deviation
SPME	Solid phase micro extraction
TBA	Tert-butyl alcohol
µL	Micro liter
USEPA	United states environmental protection agency
UV	Ultraviolet
VIS	Visible light
µg /L	Microgram per liter
µg/kg	Microgram per kilogram
µm	Micrometer

CHAPTER 1: INTRODUCTION

INTRODUCTION

1.1 WHAT IS MTBE?

Methyl Tertiary Butyl Ether (MTBE) is oxygen organic compound introduced to blend the gasoline pool since 1979. MTBE molecule synthesized from the combining reaction of the isobutylene and methanol molecules. The main objective of MTBE was applied to assist the octane level in the gasoline. In addition, the MTBE will increase the oxygen concentration to blend of the gasoline in order to meet the government obligation. The concentration of the MTBE to gasoline in order to boost octane level is about 4 to 8 % by volume [27]. Table 1 is summarized the physical and chemical properties of MTBE and the molecule is soluble to water compared with other hydrocarbon components of gasoline as tabulated at Table 2; and therefore, that behavior cause a contaminant plume to groundwater. Therefore, the environmental considerations were raised at United States to replace the MTBE by using other safer compounds such as ethanol for the gasoline oxygenate.

Table 1. Chemical/Physical Properties of Methyl-Tert-Butyl Ether (MTBE) [27].

Characteristic/Property	Data	Reference
CAS No.	1634-04-4	
Common Synonyms	MTBE; 2-Methoxy-2-methyl-propane	U.S. EPA 1993
Molecular Formula	$C_5H_{12}O$	
Chemical Structure	CH3 | CH3-O-C-CH3 | CH3	
Physical State	Colorless liquid	U.S. EPA 1993a
Molecular Weight	88.15	Budavari*et al.* 1989
Melting Point	-109^{o}C	Budavari*et al.* 1989
Boiling Point	55.2^{o}C	Budavari*et al.* 1989
Water Solubility	51.26 g/L at 25^{o}C	U.S. EPA 1993a
Density	d20/4, 0.7404 g/mL	Budavari*et al.* 1989
Vapor Density (air = 1)	3.1	U.S. EPA 1993a
KOC	12.3; 11.0 (estimated)	U.S. EPA 1993a
Log KOW	1.24	CHEMFATE 1994
Vapor Pressure Reactivity	245 mm Hg at 25^{o}C	Budavari*et al.* 1989
Flash Point	Flammable	HSDB 1994
Henry's Law Constant	5.5 x 10-4 atm m^3/mol at 25^{o}C	U.S. EPA 1993a
Odor Threshold	0.32-0.47 mg/m^3	U.S. EPA 1993c

Table 2. Physical and chemical properties of MTBE compared to BTEXs [29].

Compound	Molecular Weight (g/mol)	Water Solubility (g/L)	Henry's Law Constants, (103 atm.m3/mol	Vapor Pressure @ 20 oC (mmHg)	Log Kow
MTBE	88	48	0.55	240	0.94-1.3
Benzene	78	1.78	5.66	95.2	2.12
Toluene	92	0.52	6.71	22	2.73
Ethylbenzene	106	0.15	8.46	7	3.15
Xylene	106	0.19	7.58	10b	3.15

1.1.1 MTBE Production

In the United States the oxygenated MTBE was introduced in huge quantities and in year 1999 the USA consumed more than 200,000 barrels per day. In addition, Saudi Arabia, the MTBE was produced to gasoline blend in 2001 to replace the lead additive in gasoline blend. Saudi Arabia is the main player MTBE producers and IbnZahr produced 550,000 tons per year of MTBE. In addition, the National Methanol Company (IbnSina) was doubled methanol production to 1.2 million tons and the MTBE expected to increase capacity more than 500,000 – 700,000 tons per year.

1.1.2 MTBE Occurrence in the Environment

After discharge into air, MTBE will largely remain in the air, with smaller amounts entering soil and water. In the atmosphere, MTBE can partition into rain. However, only a small amount is removed from the atmosphere in this manner. Atmospheric transformation by hydroxyl radicals produces a number of products including the photochemically stable tertiary-butyl formate (TBF) and 2-methoxy-2-methylpropanol, which is expected to be highly reactive with hydroxyl radicals, yielding CO_2, formaldehyde, acetone and water. When MTBE is discharged into water, a significant amount is dissolved, with some partitioning into air. Partitioning into biota and into sediment is low. Biodegradability in conventional assays is limited. Generally, biodegradability is believed to be slow in the environment. When MTBE is released to the soil, it is transported to the air through volatilization, to surface water through run-off and to groundwater as a result of leaching. MTBE can persist in groundwater [24].

In comparison to petroleum products, MTBE poses additional problems when it escapes into the environment through gasoline releases; typically from gas stations' under-ground storage tank systems, above-the ground storage facilities, or pipelines. MTBE is capable of traveling through soil rapidly, is much more soluble in water than most other petroleum constituents, and is more resistant to biodegradation. As a result, it often travels farther than other gasoline constituents, making it more likely to impact public and private drinking water wells. Because of its affinity for water and, consequently, its

tendency to form large plumes, petroleum releases with MTBE can be more difficult to remediate than petroleum releases that do not contain MTBE.

The problem with MTBE is that it's contaminating the soil, air and drinking water, and may be causing health issues for people that are exposed to it. Since there is such a large amount of gasoline containing MTBE being produced and distributed every day, there are many ways for MTBE to be released into the soil, air and water. It can leak from poorly maintained underground storage tanks (USTs); accidental fuel spills; automobile and tanker accidents; motorized recreation on lakes and drinking water reservoirs; spills and drips when refueling automobiles, lawnmowers, tractors and other machines; and leaks from pipelines and improperly designed and/or poorly maintained aboveground storage tanks [10].

Although scattered incidents of localized water contamination by MTBE have been reported in the US since the early 1980s, the first report to suggest that oxygenate contamination of water might be occurring on a widespread basis came as a result of the USGS National Water Quality Assessment (NAWQA) program. This was the most comprehensive national occurrence survey of MTBE in water resources conducted to date [10, 24, and 31]. For samples taken in 1993-94, MTBE was detected (> 0.2 μg/L) much more frequently in shallow groundwater in urban areas (27 percent of sites) than in shallow groundwater in rural areas (1.3 percent) or in deeper groundwater from major aquifers (1.0 percent) [31], of the 60 VOCs measured in urban groundwater, MTBE was the second most frequently detected, ranking just behind chloroform.

In the USA, only 3 percent of the urban wells and springs sampled contained MTBE concentrations >20 μg/L.In contrast, the maximum MTBE concentration in both the shallow rural groundwater and the deeper groundwater samples was 1.3 μg/L. MTBE was detected in all eight of the urban land areas studied but in only three of the 21 agricultural areas [31].

Other regional studies have since supplemented the USGS NAWQA reports. MTBE occurrence surveys for California source water supplies have been reported by the Metropolitan Water District of Southern California (MSDSC) in Los Angeles, the University of California at Davis, and the Lawrence Livermore National Laboratory in

Livermore [8 and 10]. Drinking water supplies in Maine were also surveyed. The USGS has also studied New England groundwater, Long Island (N.Y.) and New Jersey groundwater, fractured-bedrock aquifers in south-central Pennsylvania, and MTBE occurrence in storm water in metropolitan areas. EPA has summarized the results of some of these studies in a report [33].

American Water System of the American Water Works Company performed a survey of surface and subsurface drinking water supplies. The MTBE concentrations found in the water supplies examined in this study were nearly all below 20 μg/L. This study also found that conventional water treatment processes such as coagulation/sedimentation/filtration may not be able to remove MTBE at low levels [10]. Awwa RF is sponsoring a project to develop a national database of MTBE concentrations in surface water and groundwater drinking water supplies [9].

Studies have also examined the MTBE occurrence at underground tank sites with fuel releases and demonstrated the potential for substantial MTBE contamination. It detection of MTBE was reported in more than 83 percent of the groundwater plumes monitored at more than 700 service station sites in four states [5]. About 45 percent of the sites had concentrations an excess of 1,000 μg/L. Similarly, MTBE was detected at 78 percent of the 236 leaking underground fuel tank sites in California studied by the Lawrence Livermore National Laboratory; 70 percent of the 236 sites had MTBE present at concentrations >20 μg/L and 10 percent at concentrations >10,000 μg/L [11].

In Saudi Arabia, any contamination problem to the limited groundwater sources is magnified due to the scarcity of freshwater resources. In the absence of permanent rivers or bodies of surface water and very limited rainfall, groundwater and desalinated seawater must supply the country's needs of water. One way to combat the problem of fresh water scarcity is through avoiding as much as possible any water pollution problem.

In Saudi Arabia, unfortunately, there is not much survey data published regarding the occurrence of the MTBE in the environment. This does not necessarily mean there are no contamination cases of MTBE to the groundwater. Due to the large quantities of MTBE and gasoline containing MTBE being produced and distributed every day, there is a great

potential for these compounds to reach the soil, air and water environment. In general, the great potential threat comes from contaminating the groundwater through leakage from gas stations and underground storage tanks (USTs); accidental fuel spills; automobile and tanker accidents; motorized recreation on lakes and drinking water reservoirs; spills and drips when refueling cars at the gas stations and leaks from pipelines and aboveground storage tanks.

It was found that MTBE was detected in Location a groundwater sources where samples were collected from. Other industrial sites in the Kingdom may also be contaminated where high production, loading, transporting and storing activities take place.

1.1.3 Health Effects of MTBE

MTBE is an additive mixed into gasoline supplies to reduce carbon emission. It is considered a potential human carcinogen. It is less toxic than various components present in gasoline but has the potential to cause acute damage to human life by inhalation at service stations and also its solubility in drinking water.

The toxicity data for MTBE was generated based on a controlled study of exposure of oxygenated gasoline. It has been reported that MTBE is rapidly absorbed into body thru inhalation process. Tertiary-butyl alcohol (TBA), is a metabolite forms inside the body while the person inhales MTBE. Once a person is exposed to 5.0 to 178.5 mg/m3 (1.4 to 50 ppm) of MTBE, the blood has been found to contain MTBE and TBA from 17.2 to 1144 µg/liter, and 7.8 to 925 µg/liter, respectively.

A similar study was conducted in rodents but presence of TBA was not reported. This implies that further metabolism of MTBE takes place in case rodens are exposed to MTBE. The secondary metabolism is supported by the presence of 2-methyl-1,2-propanediol and alpha-hydroxyisobutyric acid in urine of rodents. When exposed to MTBE the signs of exposure in rodents are Central Nervous System (CNS) depression, ataxia and labored respiration [12].

A separate study on rabbits has demonstrated that MTBE was “moderately” irritating to skin, causing moderate erythema and oedema. It was also irritating to the eyes of rabbits, causing mild, reversible changes. A similar study on guinea-pigs did not induce skin sensitization [12].

Similar studies were conducted on human volunteers to study controlled exposure of MTBE. The study was conducted in Alaska, New Jersey, Connecticut, and Wisconsin, USA. The reported results failed to provide an association between MTBE exposure and the prevalence of health complaints. There were no evident effects in terms of either subjective reports of symptoms or objective indicators of irritation or other effects up to 180 mg/m^3 (50 ppm) for as long as 2 h. The results demonstrate that exposure to MTBE does not cause adverse acute health effects in the general population under common conditions of inhalation exposure. However, the potential effects of mixtures of gasoline and MTBE, and the manner in which most persons are exposed to MTBE in conjunction with the use of oxygenated fuels, have not been explored experimentally.

It has been reported that when a person drinks water contaminated by MTBE, the MTBE metabolizes into formaldehyde and tertiary butyl alcohol (TBA). When MTBE gets into the air and gets into person’s lungs, it is converted into tertiary butyl formate (TBF), which causes problems in respiratory system. When (person) exposed to MTBE, the common symptoms are a long-lasting cough, sinus problems, headaches, nervousness, dizziness, nausea, insomnia, watering eyes, irritated eyes and skin rash [19].

Based on the available data, the exposure to MTBE while serving in gas stations is 12 ppm based on time-weighted average and below 1 ppm on an average basis. For the population involved in manufacturing and transportation of MTBE, this number is 700 ppm (time-weighted average) and less than 1 ppm for average exposure. These studies suggest that most people do not experience adverse health effects from MTBE present in gasoline, but the studies cannot rule out the possibility that some people do experience more acute symptoms from exposure to oxygenated gasoline than to conventional gasoline [25].

1.1.4 MTBE Regulatory Update

In December 1997, the USEPA Office of Water issued a health advisory on exposure to MTBE, primarily on taste and odor thresholds. The health advisory stated that drinking water containing MTBE concentrations in the range of 20 to 40 µg/L [or parts per billion (ppb)] would likely avoid unpleasant taste and odor effects for a large majority of people [33]. The USEPA advisory also indicated various factors influencing detection limits including individual sensitivities, water quality, and water temperature. An independent study conducted by a group of scientists using the American Society for Testing and Materials (ASTM) protocol found 15 µg/L as the geometric mean of the MTBE detection thresholds for a large group of consumer [30].

The USEPA called for significant reduction in the use of MTBE in gasoline, based on various studies. It provided the Congress with a framework for legislation that will give it the authority to significantly reduce or eliminate the use of MTBE.

In response to presence of MTBE exceeding several hundred µg/L in drinking water wells and 15 µg/L in surface of waters, the USEPA developed an action level for MTBE based on its adverse taste and odor properties in water. The State of California announced a Secondary Maximum Contaminant Level (SMCL) of MTBE at 5 µg/L based on the aesthetic properties of MTBE. Additionally, California proposed a health-based Public Health Goal (PHG) for MTBE of 13 µg/L. Subsequently, Office of Environmental Health Hazard Assessment (OEHHA) of California adopted a PHGof 13 µg/L for MTBE in drinking water based on carcinogenic effects observed in experimental animals. In December 2000, California adopted an MCL of 18 µg/L for MTBE in drinking water.

Additional studies have suggested that the benefit of use of MTBE as oxygenate in gasoline is not that important in newer vehicles. The emission system of these vehicles can be modified to achieve similar results without the addition of MTBE in gasoline. Analytical data have supported that the addition of MTBE into gasoline is the source of presence of MTBE in drinking water. MTBE ends up in drinking water supplies due mainly to poorly designed or maintained gasoline station underground storage tanks.

This being the main reason, the USEPA recommended to eliminate the use of MTBE in gasoline by 2004. Similar actions were taken by Sates such as California, New York and Connecticut to prohibit the use of MTBE and replacing it with other oxygenates such as ethanol. In June 2004, a regulatory update of MTBE usage showed that more than 19 states have either banned or reduced the usage of MTBE. (USEPA, EPA420-B-04-009). Contrary to US, European countries do not experience similar issues with the use of MTBE in gasoline. The main difference is in the amount of MTBE being added to gasoline (1.6% v/v vs. 11-15% v/v.) and the stringent requirements to maintain the underground storage tanks to hold gasoline for dispensing purposes. Additionally, in Europe gasoline is mainly dispensed under suction rather than under pressure, considerably lessening the likelihood of spills [3].

In Saudi Arabia, there are no regulations yet set for maximum allowable limits of MTBE in air or water. Therefore, the USEPA regulations will be followed as a guideline in this research study.

The Kingdom of Saudi Arabia being located in an arid region suffers from the lack of fresh water resources. In fact, the country depends primarily on the desalination of seawater and non-renewable and limited groundwater resources for its potable water supply. Due to recent wave of industrialization, especially in the area of petrochemical sector, the water source in Saudi Arabia is getting contaminated by chemicals and oxygenates such as MTBE. In Saudi Arabia, MTBE is added to transportation fuel in order to boost octane number of gasoline and to reduce carbon emission levels. As mentioned earlier, the gasoline storage tanks leak over period of time leading to release of MTBE into ground water. The transportation fuel containing up to 15% MTBE spills during loading and unloading process at fuel stations and thru transfer lines. The leaked MTBE ends up in the ground water since it is readily soluble in water and rapidly moves through soil and aquifers. The contamination raises concern about human health and safety including environmental impacts.

Several techniques have been identified to remove MTBE from water. Some of these techniques are bio-remediation [1], air stripping [6], adsorption to granular activated

carbon (GAC) [7], or use of synthetic resins. These techniques only transfer MTBE from one phase to another, without solving the basic remediation problem.

Advanced oxidation processes (AOPs) [3,17] can be applied to achieve removal of MTBE. AOP technique is applied by use of ozone/hydrogen peroxide and UV/hydrogen peroxide [17], photocatalysis with TiO_2. MTBE degradation was also investigated by other researchers under simulated heterogeneous tropospheric conditions, employing TiO_2 and iron oxides as photoactive species.

The advantage of AOPs over activated carbon and air stripping techniques is that the MTBE is degraded into other molecules, leading to complete elimination as compared to just its removal from aqueous phase. A disadvantage of any chemical or biological degradation treatment, including AOPs, is the potential for forming byproducts with higher toxicity than the original contaminant [1].

Advanced oxidation processes (AOPs) are classified basically into homogeneous photocatalysis ($UV/H_2O_2/O_3$) or heterogeneous photocatalysis (UV or VIS / TiO_2). The homogeneous photocatalysis works with high efficiency during MTBE removal but the process forms toxic by-products such as butyl alcohol (TBA) and tert-butyl formate (TBF) and bromate.

Metal Oxides such as TiO_2 and ZnO, due their optoelectronic property are widely used in photooxidation reactions under UV light. These catalysts are highly stable, free of hazardous risks, and inexpensive. They exhibit a very high photocatalytic activity under UV irradiance due to their wide band gap. Unfortunately, less than 7% of sunlight is composed of UV light while visible light makes around 46% of sun light. Due to the requirement of UV light to function properly, scientists conducted research to find metal oxides that work well under sunlight to induce photocatalytic reaction. It has been reported that TiO_2 is the most widely used metal oxide catalyst for photocatalytic reactions and degradation of organic pollutants but in some cases ZnO is preferred due to its high quantum efficiency [43].

Certain catalyst such as Fe_2O_3 have narrow band gap which can work under visible light but are not suitable due to their instability under aqueous conditions. The narrowing of the wide band gap of metal oxides was achieved by doping catalysts with different metals or non-metals, surface modification, creation of oxygen vacancies, co-doping of non-metals, transition metals coping and spatially structured and chemically modified visible-light active titanium [43].

1.2 OBJECTIVES

The main objective of the study was to assess the treatability of water contaminated by MTBE by using the method of the visible light photooxidation through selected heterogeneous catalyst with co-catalysts under room temperature without adding the hydrogen peroxide as oxidant for MTBE oxidation. The specific objectives were as following:

- Develop visible light reaction condition for MTBE
- Develop SPME technique incorporated with GC-MS to assist the MTBE photooxidation study
- Perform catalyst syntheses as following:
  - Synthesis several concentrations from 0.5% to 2.5% of noble metal Ru in WO_3
  - Synthesis several concentrations from 0.5% to 2.5% of noble metal Ru in nano WO_3
  - Synthesis several concentrations from 0.5% to 2.5% of noble metal Pt in WO_3
  - Synthesis several concentrations from 0.5% to 2.5% of noble metal Pt in nanoWO_3
- Determination MTBE degradation and hydrocarbon by-products from photooxidation.

CHAPTER 2: LITERATURE REVIEW

2. LITERATURE REVIEW

2. 1 Photodegradation of methyl tert-butyl ether (MTBE)

Literature reviews for several photodegradation treatment methods for MTBE from water stream were studied. The review highlighted the important aspect for of photodegeradation, oxidation of MTBE treatment with and without catalysts.

Qinhai et al conducted the study of MTBE degradation based on UV advanced oxidation processes (AOP) and compared it to the Photodegradation of MTBE by UV/H_2O_2 without catalysts and UV/TiO_2 catalysts without hydrogen peroxide. It was done to evaluate the removal efficiencies and optimal conditions for the photodegradation of methyl tert-butyl ether (MTBE). However, the authors adjusted the pH of wastewater contaminated by MTBE in order to perform the Photodegradation. Their work revealed the optimal conditions at an initial MTBE concentration of 1 mM were acidic at pH 3. At 15 mM H_2O_2 dose in UV/H_2O_2 system was found the best. The UV/TiO_2 without hydrogen peroxide system at pH 3.0 the optimum amount of TiO_2 was 2.0 g/l for Photodegradation of MTBE [28].

The work concluded that the pseudo first-order rate constants linearly increased with the increase in the molar ratio of [H_2O_2] to [MTBE] in UV/H_2O_2 system and linearly increased with the decrease in MTBE in UV/TiO_2 system.

The oxidation of organic compounds by free hydroxyl radical (*OH) produced from UV-irradiated the hydrogen peroxide is well established [28]. Hydrogen peroxide absorbs the light energy from UV irradiation and then the bond of (O–O) is ruptured leading to the production of activated $^{\cdot}OH$ and the atomic oxygen (equation (1)). With increasing hydrogen peroxide concentration an increased energy absorption and production more

*OH and that will increase the oxidative destruction of MTBE and MTBE by-product. This is shown in the following reactions:

$$H_2O_2 + h\nu \rightarrow 2\ {}^{\cdot}OH \qquad \text{equation (1)}$$

The consumption of hydrogen peroxide during the photooxidation of MTBE was experimentally measured (equation (2)) in a system containing initial concentrations of 1 mM MTBE and 10 mM H_2O_2 [28].

$$RH + {}^{\cdot}OH \rightarrow H_2O + {}^{\cdot}R \rightarrow CO_2 + H_2O \qquad \text{equation (2)}$$

Jia Lu performed the treatability of methyl tert-butyl ether (MTBE) in five ground waters by using several oxidation methods and the UV/H_2O_2 advanced oxidation process was one of the methods [13]. The UV system used was a 1-kW medium-pressure mercury vapor arc lamp and the pH was controlled to 7 and 9 (±0.1) in these experiments to examine the influence of pH on hydroxyl radical scavenging and overall process efficiency. The study concludes the advanced oxidation provided the lowest treatment costs for four of five ground waters. However, an ineffective for a high chemical oxygen demand of ground water led to poor MTBE treatment. The UV/H_2O_2 process was more efficient at pH 7 versus pH 9. However, the study applied high ratio of hydrogen peroxide from 25 to 100 to MTBE concentration in order to degrade the MTBE from groundwater. The degradation of MTBE by UV/H_2O_2 and UV/TiO_2 and the degradation of MTBE by UV/H_2O_2 and UV/TiO_2 photocatalytic [2] followed a first-order model with apparent rate constant of 1.31×10^{-1} and 1.21×10^{-2} min^{-1}, respectively. The catalyst of TiO_2 loading was found to be 1.5 g/L for 10 ml/g of MTBE concentration. In addition, the authors compared between MTBE degradation rates of UV 254 and UV 365 and they found the light with 254 nm wavelength had more effectiveness on the degradation of MTBE than that of 365 nm as illustrated in Figure 1.

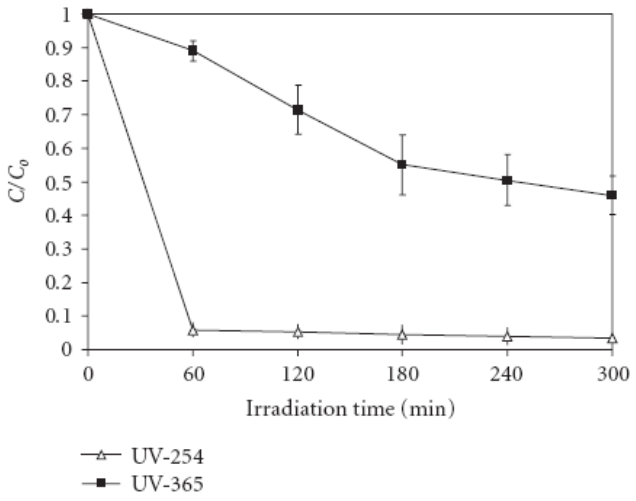

Figure 1. The comparison between degradation rates of UV254 and UV365 via TiO_2 catalysts [2].

Comparative study of MTBE decomposition through catalysts of $Au/TiO_2–Al_2O_3$ and Au/TiO_2 was performed by Araña [14]. MTBE photo-decomposition as a function of time under visible irradiation on gold photocatalsyts is shown in Figure 2. The Au/TiO_2-Al_2O_3 had a complete decomposition of MTBE compared to Au/TiO_2 catalysts decomposed MTBE about 50% during the same time interval. In addition, the catalysts with gold particle size ≤7.5 nm showed higher activity than the catalysts with gold particles >7.0 nm as illustrated below.

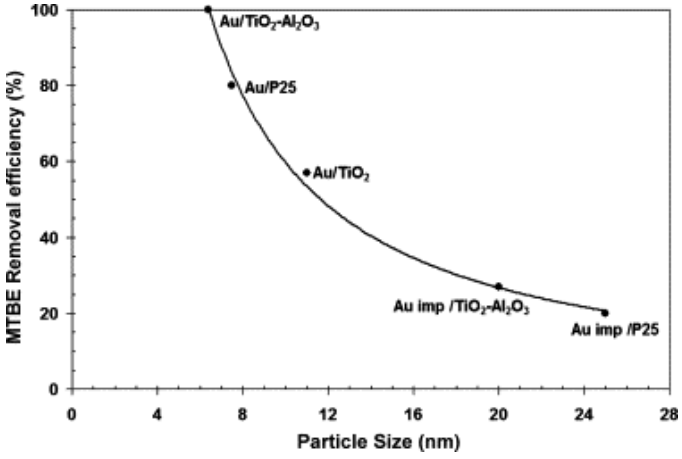

Figure 2. MTBE removal efficiency as a function of the gold particle size [14].

Another approached for MTBE treatment was investigated Araña [14]. They studied the photocatalytic techniques with catalysts of TiO_2 (Degussa P-25) and TiO_2 loaded with Cu (Cu-TiO_2). The experiments were carried out in a continuous reactor device at 35°C adjusted to pH 5 by adding diluted sulfuric acid and the vessel is continuously air-bubbled at a flow rate of 10 cm^3/min. The air containing water and MTBE or others mixtures vapor introduced in reactor 15 cm long, 4 mm diameter cylindrical Pyrex glass reactors containing the catalyst and it exposed to the UV light. The results showed degradation the tested compound and the reactor with Cu-TiO_2 has been more efficient than that with TiO_2 at the degradation and degradation of MTBE.

A researcher noticed that the MTBE is difficult to treat economically with conventional techniques [3]. However, it has been found to be readily degraded photocatalytically. They studied TiO_2 slurries and under the experimental conditions. The MTBE compound degradation proceeded with an initial pseudo first-order rate constant of 1.2 x 10^{-3} s^{-1} and the primary by-products of this reaction have been identified as *t*-butyl formate and *t*-butyl alcohol. The by-products are also readily degraded photocatalytically, although at slightly slower rates than MTBE. Mass balance calculations have shown that MTBE is virtually completely mineralized [3].

Another work done by Qinhai, where he mineralized MTBE into CO_2 via the UV/H_2O_2 system or in UV/TiO_2 system. During the photodegradation they identified the intermediate products of MTBE by gas chromatography–mass spectrometry (GC–MS). The major intermediate was tertiary butyl alcohol (TBA) base peak at *m*/*z* of 59 corresponds to a possible fragment ion either $CH_3O–C=O^+$ or $^+OC_3H_7$ and formic acid [26]. Park et al studied the mechanism of degradation of MTBE [28]. The generated hydroxyl radicals from hydrogen peroxide attacks on the methoxy group in the MTBE structure dominated and proceeded through tert-butyl formate (TBF) as an intermediate and proceed to form 2-methoxy-2-methyl propionaldehyde (MMP). Carbon dioxide is final product through acetone which was shown easily converted to CO_2 as illustrated in Figure 3.

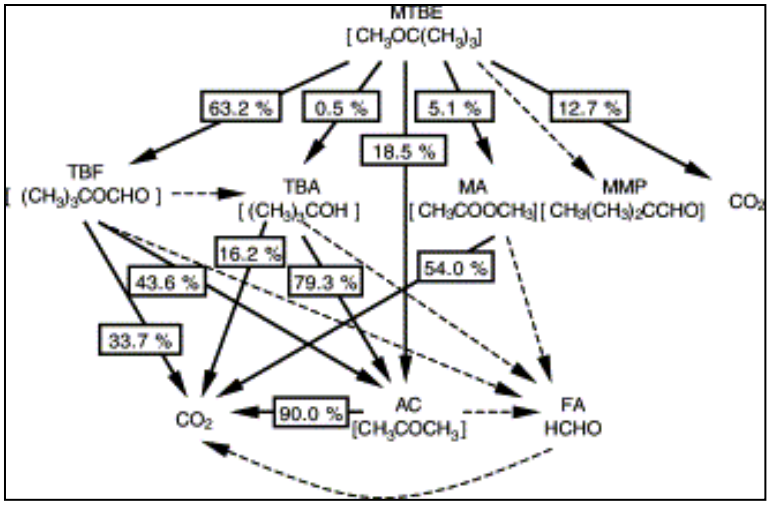

Figure 3. MTBE degradation and by-products and the percentages given refer to the relative importance of pathways [28].

2.2 Catalytic combustion oxidation of methyl-*tert*-butyl-ether (MTBE)

Figure 4 shows the catalytic combustion oxidation of methyl-*tert*-butyl-ether (MTBE) in the gas-phase from an aqueous solution by simulating actual remediation conditions. The solution of MTBE was sparged with an oxygen/helium gas, at a ratio of 1 to 4. The sparged gas stream of MTBE and water vapor was passed over studied catalysts Pt/Rh and Pd conjuncted with $La_{1-x}Sr_xMnO_3$ [21]. The results were compared to a commercial catalyst which contained a higher loading of Pt and the combustion to CO_2, water was observed in all cases. The catalyst with the lowest loading of Pt/Rh achieved the lowest temperature for complete oxidation of MTBE and its by-products at the lowest temperature. Then the MTBE decomposes to isobutene and methanol, followed by combustion by a sequence of reactions and at space velocity of 62,000 h^{-1}, total conversion can be obtained at temperatures of 300°C or lower.

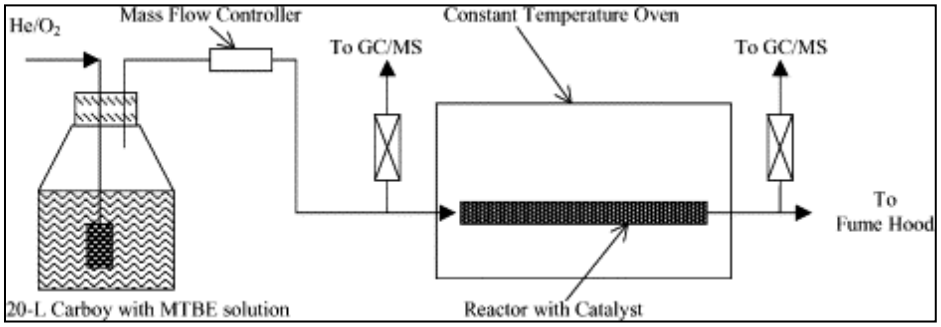

Figure 4. The Experimental set-up for catalytic combustion oxidation [21].

In the summary the photooxidation of MTBE with TiO_2 without hydrogen peroxide oxidation agent would lead to many by-products and these by-products are difficult to be mineralized. Nevertheless application of photooxidation without proper catalysts also will require high dose of hydrogen peroxide and adjustment of pH level. The Table 1 summaries the catalysts for the photooxidation and the results were obtained. Other study applied similar methods of other authors and many by-products were not reported [29]. In addition, the literature review were not cleared how MTBE would fully mineralized and other reported these compounds are slow to be removed from water stream.

2.3 Various ways for the making of TiO_2 and ZnO Visible Light Active

The adaptation of metal oxides to shift the band edges from UV region toward the visible light region was reviewed [43]. Several techniques and methods were tested in order to modify the visible light by using a surface modification through organic materials with selected semiconductor coupling. The dye sensitization was subjected for surface modification and the molecules of dye were adsorbed, in addition, it the dye can be connected with metal oxide surface as well through weak Van Der Waals forces such as methylene blue (MB) and eosin-Y Figure 5.

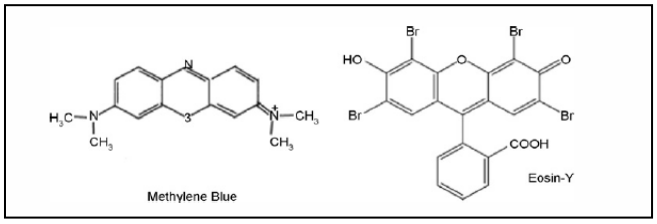

Figure 5. Structure of methylene blue and eosin-Y [43].

The presence of these dyes on the surface of metal oxides helps to induce photocatalytic reactions because they facilitate the movement of electrons from the dye molecules to the semiconductor e.g. TiO_2. The potential of the lowest unoccupied molecular orbital (LUMO) of the dye is more negative than the conduction band of the host semiconductor. Therefore, electrons are injected to the conduction band of the semiconductor when the dye is excited by visible light, Figure 6. Electrons are then scavenged by molecular oxygen to form superoxide racial (O2•−) and hydrogen peroxide radical (•OOH).

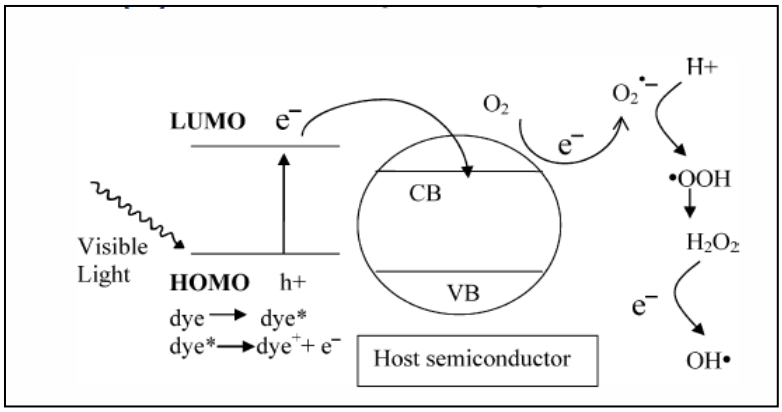

Figure 6. Activation of the semiconductor band gap by dye sensitization [43].

It was concluded that dye sensitization is a very useful method for the activation of wide band gap semiconductors but due to the potential of frequent desorption of dye molecules, they cannot be reliable to be used for long term photocatalytic reactions. To avoid this dilemma, other techniques such as surface-complex assisted sensitization, polymer sensitization and semiconductor coupling for surface modification can be used. At the present time, no detailed studies were conducted on the efficiency of these methods on photodegradation reactions therefore they won't be a part of the study

regarding MTBE removal. In addition, band gap modification by creating oxygen vacancies and oxygen sub-stoichiometry, making of oxygen vacancies crystal structures was found to be a good technique to increase the sensitivity of metal oxides towards visible light. When oxygen vacancies are created in the grain boundaries of samples, they produce new states below the states at the conduction band of the metal oxide with energy of less than 1 eV. As a result, visible light absorption edge shifted λ= 350 nm to λ=550 nm. The only drawback of this technique was the restricted control it gives towards electronic and optical properties of the meal oxide. The co-doping of metal oxides by non-metals was studied and they found that doping TiO_2 with two non-metals at the same time e.g. S and N- TiO_2 resulted in a catalyst with a higher response to visible light than pure TiO_2, N-TiO_2 or S-TiO_2 [45].

Doping of metal oxides by transition metals, non-metals and spatially structured and chemically modified vis-light active Titania. These techniques were also evaluated during the study, the authors of this study came to an end that co-doping of semiconductors by non-metals resulted in a high photocatalytic potential and a higher visible light activity.

2.4. Using Element-Loaded TiO_2 for Visible-light -induced Photocatalysis of MTBE

The previous study of the photocatalytic activity of non-metal loaded TiO_2 [45] showed that TiO_2 is highly active under UV light, because it exceeded the band gap energy of 3.0 - 3.2eV. In order to utilize the abundance of visible light, doping technique was used due to its rule in elevating and enhancing the absorbance of visible light in metal oxides. Doping TiO_2 with non-metals enhances both light absorption and photocatalytic activity. Thereby, sulfur (S) and nitrogen (N) [45] which were examined during this study, S-loaded and N-loaded TiO_2 demonstrated a very high absorption and potential towards the visible light and showed good photocatalytic activity. Using a diffuse reflectance UV-VIS-NIR-spectrometer, the absorption edge for S-loaded and N-loaded were found to be shifted from UV to visible light region λ=720 nm and λ=400-425 nm respectively, results were quite high compared to unloaded TiO_2 where λ=410 nm as shown in Figure 7.

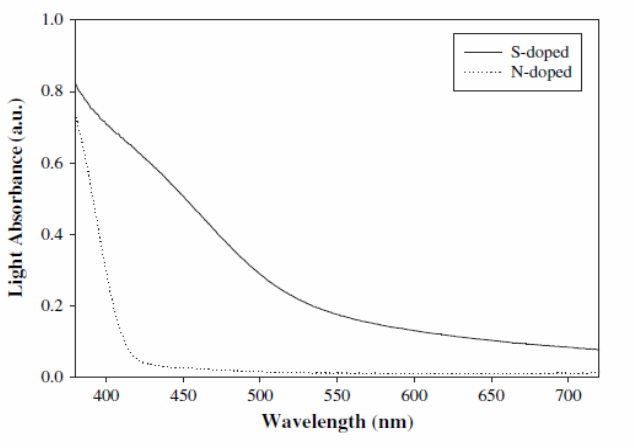

Figure 7. The UV-visible absorbance spectra of S- and N-loaded in TiO_2 [45].

Furthermore, the degradation efficiencies of this study show that 75% of the MTBE degradation efficiency was achieved using S and N loaded inTiO_2 as illustrated in Figure 8. These results were similar to the studies that used TiO_2 and UV [45]. It is important to know that the resulted by-product is negligible due to the presence of CO in the indoor concentration.

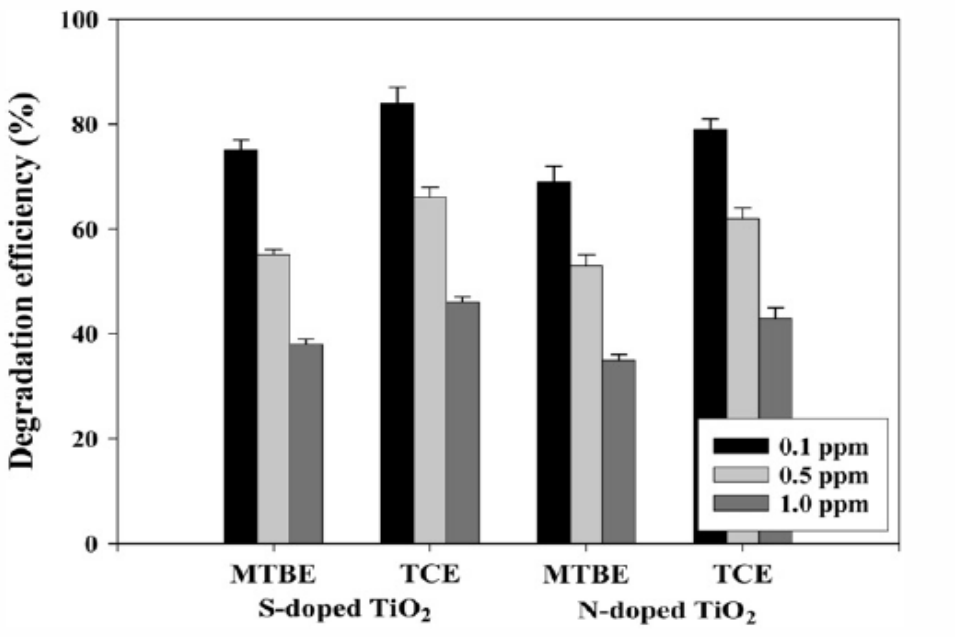

Figure 8. MTBE degradation using loaded TiO_2 [45].

2.5. Photocatalyst Degradation of Organic Pollutants under Vis-light Using Modified TiO_2

Wu et. al evaluated photoactivity of loaded TiO_2 with both boron and carbon using sol-gel followed solvothermal process for the preparation of B and C TiO_2. X-ray diffraction (XRD), X-ray photoelectron spectroscopy (XPS) and some other analysis showed that B and C both have enhanced the visible light absorption λ= 400-500 nm [44]. The diagram in Figure 9 exhibits how the band gap energy decreases with the amount of added Boron making the product for more active under visible light energy.

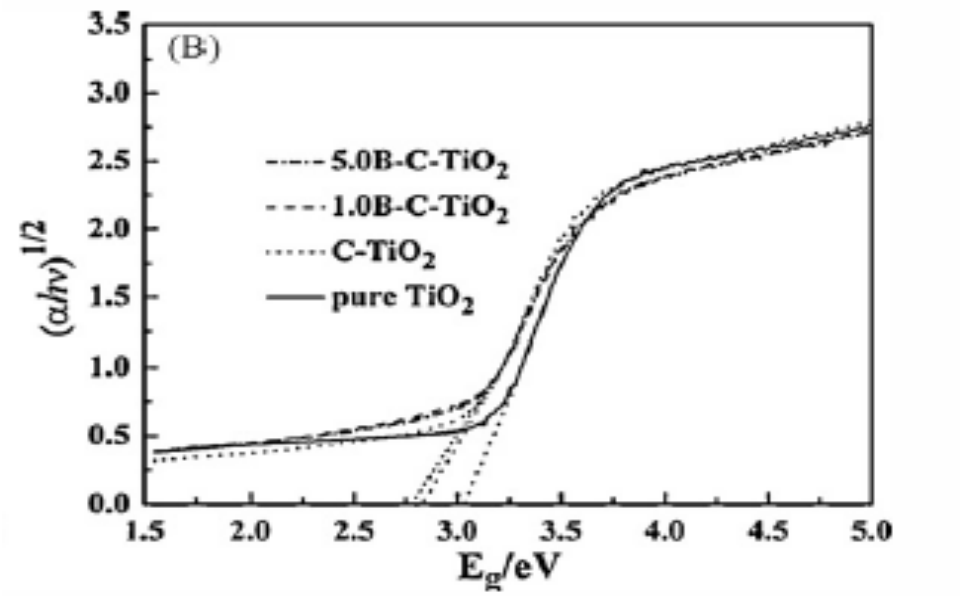

Figure 9 Effect of added Boron on the energy gap [44].

In addition, the acid orange 7 was used to evaluate the photocatalytic activity of B and C TiO_2 under visible light. Moreover, it was found that calcinated C-TiO_2 absorbs light at λ = 400 -600 nm, Figure 10 [44]. The activated TiO_2 under visible light was utilized for the removal of MTBE and as suggested by Lamber and co-workers [44] that B-loaded TiO_2 poses the potential to absorb high amounts of visible light which at the end elevated the photocatalytic activity for the degradation of MTBE.

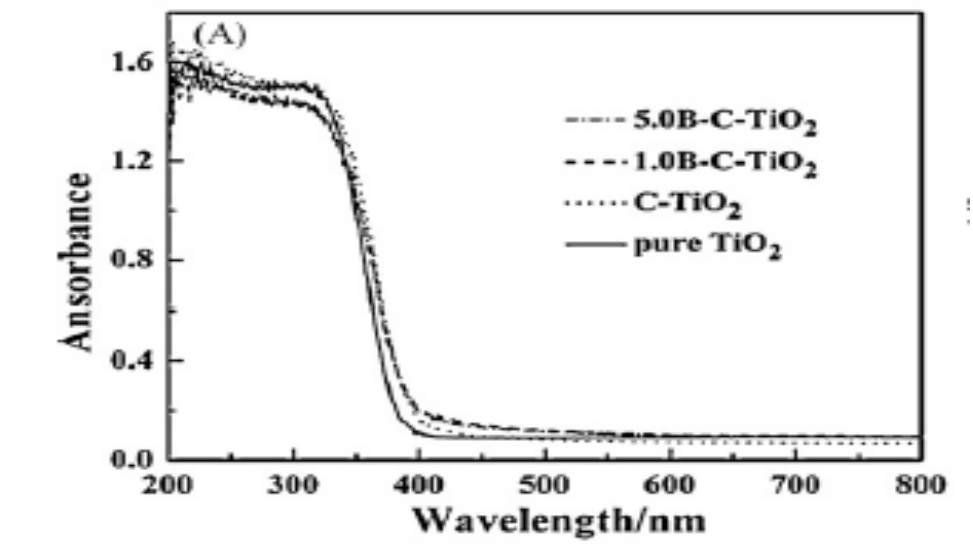

Figure 10 Spectra of C-TiO_2 with different concentrations of B doping [44].

Table 3 Summarizes previous studies conducted on the photooxidation of MTBE by UV and under visible light. Only handful of papers was found using visible light for the photooxidation of MTBE. Jo et al [46] reported using nitrogen and sulfur loaded on TiO_2 under visible light to achieve 75% degradation of MTBE. Therefore the current research is geared towards the photooxidation of MTBE under visible light utilizing the best combination of catalysts and photooxidation conditions.

Table 3.The summary of the photoxidation of MTBE under various catalytic conditions [45].

Author	Catalyst - Oxidant	Conclusions	Reference
Hu *et al.*	UV/TiO_2 and UV/H_2O_2	UV/TiO_2 load was high amount of catalysts Adjusted water to pH 3 by addition acid	[26]
Lu *et al.*	No catalysts only UV/H_2O_2	hydrogen peroxide from 25 to 100 to MTBE concentration	[14]
Asadi et al.	UV/H_2O_2 and UV/TiO_2	The study need to be examined	[02]
González et al.	No oxidation used and Au/TiO_2–Al_2O_3 and Au/TiO_2	Longer time and decomposition of MTBE took 150 minutes	[18]
Barreto et al.	No oxidation used and TiO_2	The by-products are also readily degraded photocatalytically,	[03]
Preis et al.	No oxidation used and TiO2	Many by-products	[29]
Mitani et al.	Oxygen with Pt/Rh and P	Treatment of the gas phase of MTBE	[21]
Sham Rehman, R. U.	Vis/N and S TiO_2	Absorption edge is highest amongst other catalysts.	[43]
Wan-Kuen Jo, Chang-Hee	Vis/S-TiO_2 Vis/N-TiO_2	λ of S-TiO_2 = 720 nm λ of N-TiO_2 = 425 nm	[13]
Hu *et al.*	UV/TiO_2 and UV/H_2O_2	UV/TiO_2 load was high amount of catalysts Adjusted water to pH 3by addition acid H_2O_2 was 15 times to remove 1 MTBE	[26]
Barreto et al.	No oxidation used and TiO_2	The by-products are also readily degraded photocatalytically, although at slightly slower rates than MTBE	[06]

CHAPTER 3. RESEARCH METHODOLOGY

3. RESEARCH METHODOLOGY

3.1 Chemical and Materials

The study utilized tungsten (VI) oxide WO_3, which was received from Aldrich at 99% purity. Hydrogen hexachloro platinate (IV) hydrate from Aldrich at 99.9995% purity and Ru (III) chloride hydrates from Aldrich at 99.999% purity, were used for platinum and ruthenium precursors, respectively. MTBE was obtained from Bulvdick and Jackson and was used as such without any further purification Ruthenium (III) received from Aldrich at 99.9% purity.

Solid phase microextraction (SPME) 100 µm Polydimethylsiloxane (PDMS) from Supleco was used as sorbent for the extraction of the analyte. 500 ml size reactor was used with halogen lamp 75w from Halolux, which emits 95% of light within the infrared region.

3.2 Gas Chromatography/Mass Spectrometry (GC/MS)

Agilent Model 7890A Gas Chromatography/Mass Spectrometry detector (GC/MS) instrument with column HP5-MS, 50 m x 0.25 mm i.d., 0.25 µm film thickness. The GC oven was operated at a gradient temperature: 45 ^{0}C held for 1 minute then ramped to 60ºC @ 5ºC/min. and then ramped to 140ºC @ 20 ºC/min . The range of operation (40-140 ºC) was used for the analysis of organic chemical mixtures in order to determine the mass ions of molecules. The column was operated under a constant carrier helium gas flow of 1.4 mL/min. Chemstation software was used for data processing. MTBE was identified by its mass spectra and by matching its retention times (6.2 min) with that of the pure MTBE sample. Two quality control samples were injected during the analysis sequence in order to monitor the performance of the developed analytical method. The sample is injected into heated sample inlet of the GC/MS for 1 minute to obtain the required results. The total run time is around 9.0 minutes for the single analysis. Figure 11 illustrates the GC/MS system.

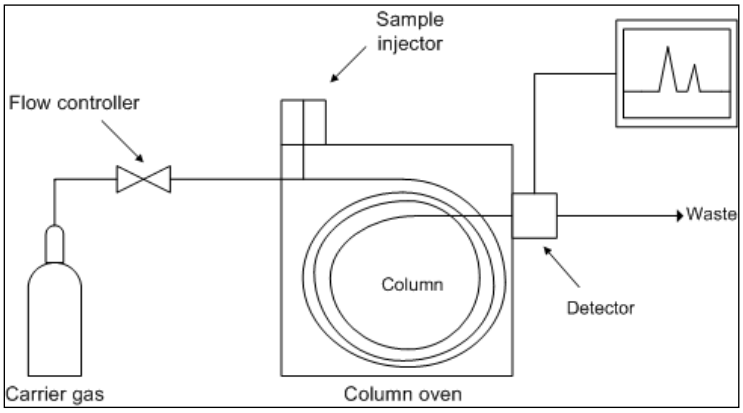

Figure 11. Gas Chromatography/Mass Spectrometry (GC/MS) diagram [48]

3.3 Solid-phase micro extraction (SPME)

Solid phase micro extraction (SPME) method is a new extraction technique method for hydrocarbon extraction. For example, the SPME fiber type 100 µm PDMS (polydimethylsiloxane) is common used for hydrocarbon extraction and adsorb the molecules in gas as head space extraction or adsorb hydrocarbon molecules from aqueous phase. The adsorbed molecules are known extraction into the fiber is proportional to concentration as long as the equilibrium is reached at the known time of SPME extraction. In the case of the MTBE extraction by SPME a 5 mL collected from visible reactor and placed in sample vial and then the SPME was placed in vial for 10 min time keeping the fiber above the liquid level to extract the molecule from head space. The molecule of MTBE was absorbed and extracted for each sample, After extraction, the SPME fiber was transferred to the hated injection port of GC/MS at 200 ^{o}C, where desorption of MTBE was taken place from SPME and moves out to column chromatography of GC/MS.

3.4 Preparation of stock solution

MTBE stock solution of 1000 ppb was prepared by dissolving 0.00025 g of MTBE in 2.0 L of raw water, and then 100 ml of 1000 ppb MTBE stock solution was added in 1 L to prepare 100 ppb MTBE stock solution which will be used for the reaction.

3.5 Reactor

The study was utilized a visible light in 500 mL reactor, the lamp introduced into the immersion wall photochemical reactor made of Pyrex glass equipped with a magnetic stirring bar, the circulating water into jacket glass wall with opening for supply of gases. The schematic of the photoreactor is shown at Figure 12 for irradiation experiment.

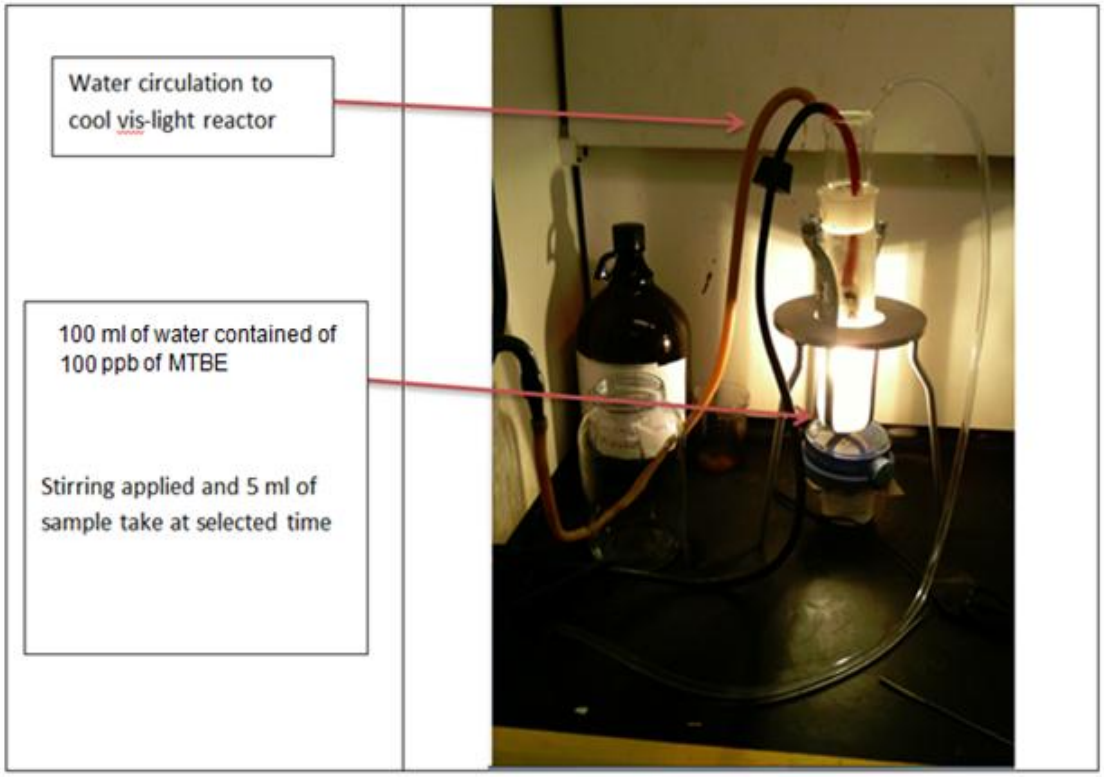

Figure 12. Photo-reactor set-up for photocatalysis of contaminated water. The prepared catalysts were evaluated in term of the degradation of MTBE under visible light. 100 mg of the sample was added to the reactor of 500 mL size containing 100 mL of MTBE stock solution at 100 ppb. Halogen lamp was placed in the reactor attached to water flow cooling system. The mixture was stirred gently; 5 mL of the sample was taken at 0, 30, 60 and 240 min.)

3.6 Preparation of MTBE for Baseline stability and Photooxidation experimental:

The following illustrates the preparation for the Photooxidation experiments.

3.6.1 Extraction Profile of SPME Fiber

A 500 ppb solution of MTBE was prepared to study the extraction profile of SPME fiber. A 100 µm thick PDMS fiber from Supleco was used for this purpose. The fiber was placed into a 10 mL solution of 500 ppb MTBE for 5, 10 and 20 min. and the amount extracted were analyzed by headspace GC/MS technique. In each case three measurements were taken.

3.6.2 Effect of evaporation of MTBE in stirring reactor without catalysts and halogen lamp treatment

A 500 ppb of MTBE standard was placed in a stirring reactor in absence of catalysts and halogen lamp. The experiment was conducted to establish the loss of MTBE with time while under stirring conditions. The samples were collected at 60, 150, and 240 min (1, 1.5, and 4 hrs) and analyzed using SPME 100 µm PDMS fiber using headspace analysis under GC/MS technique.

3.6.3 Effect of evaporation of MTBE in stirring reactor in presence of halogen lamp treatment

A 500 ppb of MTBE standard was treated with halogen lamp. A water solution of 100 contained 500 ppb of MTBE. A sample of this mixture was analyzed for presence of MTBE using SPME technique. 100 µm fiber containing PDMS was used with an extraction time of 10 min; the GC/MS analysis was performed using headspace technique.

3.6.4 Effect of halogen lamp and catalyst

A 100 mL of 100 ppb stock solution of MTBE was added to the reactor in presence of halogen lamp and catalysts. A small amount of WO_3 catalyst was added to the stock solution with gentle stirring. Samples were collected at different intervals using SPME

fiber and analyzed under GC/MS instrument using headspace analysis technique. Replicate analyses were conducted for each sample and average peak area was reported. A similar experiment was conducted in presence of halogen lamp. Samples were taken at regular interval and analyzed using SPME fiber in conjunction of GC/MS headspace analysis.

3.7 Catalyst preparation

3.7.1 Synthesis of nano WO_3:

Dissolve sodium tungstate in 100 mL of distilled water (6.6 g, 0.2 mole) and acidification will be done by adding HCl to get a pH of 1 to obtain a white precipitate, and dissolve by adding oxalic acid (0.4 g in 30 mL DW, 0.1 mole). As a result, a transparent solution is obtained. The solutions were transferred into 100 mL Teflon-lined stainless steel autoclave and maintained at 180 ^{o}C for 24 h to get the final product.

3.7.2 Synthesis of noble metals (Ru and Pt) loaded on WO_3

The photo deposition of Ru loaded on WO_3 was prepared by 500mg of WO_3 and place 100.0 mL of distilled water in a beaker. Then, add 2.5mg of Ru to the beaker. After that, the solution bubbled with nitrogen for 30 minutes to remove the excess of O_2 while stirring slowly. Then, 5.0 mL of methanol was added. The solution then transfer to the reactor and turn the lamp for 6 hours while stirring via a magnetic stirrer and a stirring plate. After the reaction took placed, co-catalyst Ru/WO_3 centrifuging the solution for 30 minutes and dries the catalyst at ~700 ^{o}C in the oven. Similarly the $Pt/WO_3$was prepared.

3.8 Sample Characterization

3.8.1 Catalyst Characterization by X-ray Diffraction Technique

X-Ray Powder Diffraction (XRD) technique is an excellent analytical technique used for phase identification of a crystalline material [38-42]. XRD identified compounds, whereas X-Ray Fluorescence (XRF), induced-coupled plasma and atomic absorption techniques only provide elements.

3.8.1.1 XRD Sample Preparation

The synthesized catalyst powders were manually ground in an agate mortar and a pestle for several minutes to achieve fine particle size and adequate intensity reproducibility [38-42]. Then, the fine powder was mounted into the XRD sample holder by back pressing.

3.8.1.2 XRD Data Measurements

Table 4 lists the XRD pattern measurement conditions. The continuous-scanned patterns were measured with a PANalytical X′PERT XRD diffractometer. The basis on which various conditions/settings were selected is as follows [41]:

- Data were not recorded below 10° in 2θ because Bragg peaks do not occur below this angle for the materials considered, and data were collected to 2θ = 90° because the Bragg intensities of the samples were insignificantly beyond this angle.
- Position sensitive detector (PSD) X′Celerator was used with a scanning step time of 9.73 seconds ensured reasonable intensity counting statistics. PSD length in 2θ was 2.12°, with irradiated and specimens lengths were 10 mm and 10 mm, respectively.
- A detector step size of 0.008 was employed to provide adequate sampling of the peaks [full width at the half maximum (FWHM) approximately 0.11° - 0.34°].

All of the samples were spun during the data collection to improve particle counting statistics; thereby the intensities are not dominated by a small number of crystallite.

Table 4. XRD pattern measurement condition [41].

Name	Description
Instrument	PANalytical X′PERT PRO MPD
Radiation	Cobalt-anode tube operated at 40 kV and 40 mA
	Wavelength: $K\alpha_1$ = 1.78901Å, Co $K\alpha_2$ =1.79290Å, $K\alpha_2$ / $K\alpha_1$ ratio = 0.50
Optics	Bragg–Brentano, measuring circle diameter = 480 mm
	Divergence slit type: automatic
	Irradiated length = 10 mm and Specimen length = 10 mm
	Distance Focus to Divergence Slit = 100 mm
Specimen	Holder: circular format, diameter = 20 mm
	Rotation "on" for all measurements
Detector	PSDX'Celerator
	PSD mode: scanning; PSD length in 2θ = 2.12°
Acquisition	Angular range in 2θ: 10° - 90°
	Step size: 0.008°
	Scanning step time: 9.7282 s

3.8.1.3 Phase identification

For phase identification (or qualitative analysis), the PANalytical High Score Plus software, combined with the International Center for Diffraction Data (ICDD) and powder diffraction file (PDF) database of the standard reference materials, were used. The phase identification results (or chemical compounds) along with the identified mineral reference was considered.

3.9 Environmental scanning electron microcopy (ESEM)

Environmental scanning electron microcopy (ESEM) with integrated energy dispersive X-ray spectroscopy system (EDS was applied to perform topographic and elemental analyses on the studied samples. In brief, ESEM is an analytical instrument that uses electrons instead of visible light to form magnified images of an object by scanning it with a high-energy beam of electrons in a raster scan pattern. The environmental scanning electron microscope is the natural extension of the conventional scanning electron microscope (SEM) and incorporates all of the conventional functions of SEM with addition capabilities. Secondary electron and backscattered electron images along with EDS spectra were acquired from different parts in the examined samples. The samples were mounted on ESEM stub using double sized conductive carbon tapes and then inserted into the ESEM chamber for examinations.

3.10 Photooxidation reactor

The photocatyltic activities of samples were evaluated in term of the degradation of MTBE under visible light illumination. The photocatalyst powder (100 mg) was dispersed/ added to the reactor containing 100 ml of MTBE stock solution, 100 ppb in concentration. Halogen lamp was placed in the reactor attached to water flow cooling system. The mixture was stirred gently, samples were taken at different time scales; the first sample (0 min) was taken after 30 min of constant stirring with the lamp turned off. Then lamp was switched on and the second sample was taken after 30 min and the other samples were taken after 2, 3 and 4 hours, respectively.

The efficiency of the used catalyst was evaluated via GC-MS through the use of SPME technique. SPME was placed in each vial for 10min to collect the vapors of MTBE with extra care to keep the fiber above the liquid level. Then, it was injected to the GC-MS instrument to obtain the required results with an estimated run time of around 9 minutes for the single analysis. Every sample was run twice to ensure the stability of the results. Between every run, the fiber was dipped in water and then injected to the GC-MS, thus to make sure that there is no MTBE contamination coming from the previous sample.

CHAPTER 4. RESULTS AND DISCUSSION

4. RESULTS AND DISCUSSION

This study was conducted in two phases; first to investigate the experimental stability of analytical technique involving SPME in conjunction with headspace analysis using well known GC/MS technique. The advantage of SPME is to avoid difficult extractions such MTBE from water phase into simple method at a fast rate. Additionally, the SPME technique is an extraction without the use of any solvents with detection limits reaching up to parts per trillion (ppt) levels for certain compounds.

The second phase of the study was associated with the use of various catalysts and the development of optimum catalyst/catalyst composition for the degradation of aqueous MTBE in presence of visible light.

4.1 Baseline and experimental stability

4.1.1 Extraction kinetic profile of aqueous MTBE in water:

A 500 ppb solution of MTBE was prepared to study the optimum extraction time when the extractions reach the equilibrium. The results of extraction time are reported in Table 5. The chromatography peak area response was recorded in each case. Chromatography peak area response for SPME extraction for 10 minutes was found to be the best with a coefficient of variation 6.8%. In case for 5 minute and 20 minutes the RSD were found at 45.3 and 11.1 respectively. Figure 13 illustrates these findings as a graphical representation.

Table 5. SPME extraction time visible light the MTBE response by MSD.

	chromatography peak area response			statistic		
Extraction time	Run 1	Run 2	Run 3	mean	s	RSD %
5 min	1224409	689841	519428	811226	367832	45.3
10 min	5799252	5067552	5358047	5408283.7	368428	6.8
20 min	4836210	5322006	6023250	5393822	596770	11.1

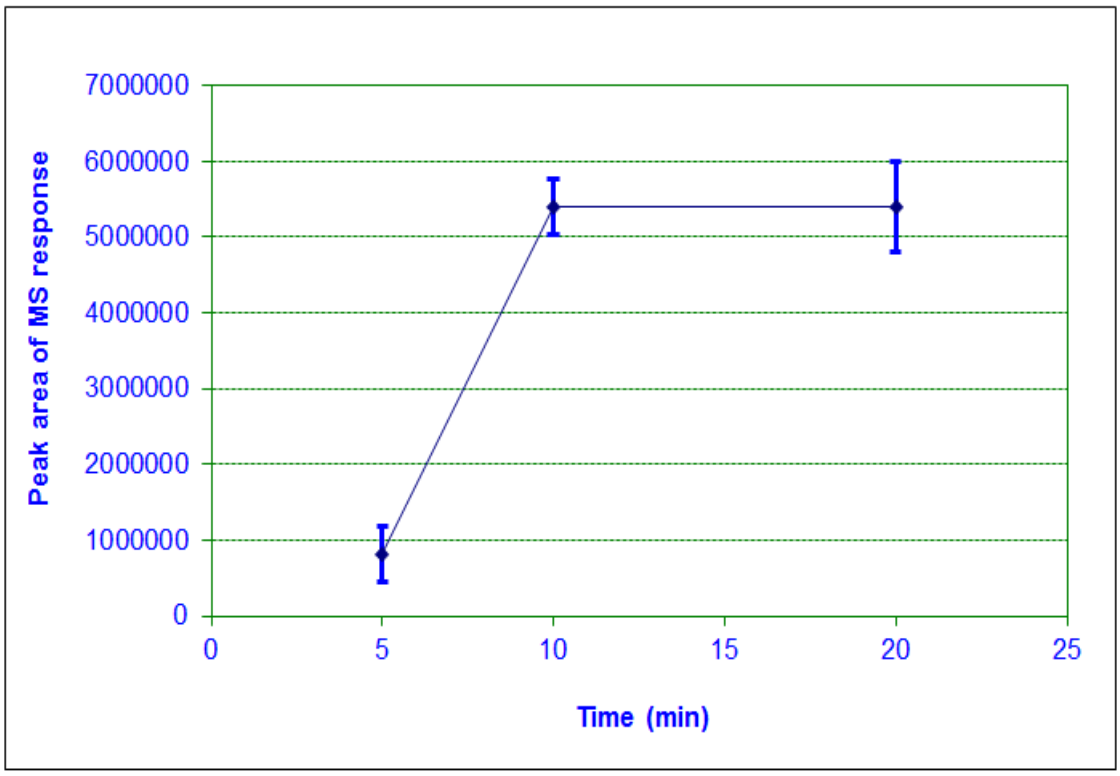

Figure 13. Shows the extraction kinetics of aqueous MTBE on coated SPME. A 500 ppb solution of MTBE was analyzed for the evaporation effect during the stirring reactor without halogen lamp and catalysts. The samples were collected at 5, 10, and 20 min intervals. Peak area response using SPME extraction technique for 10 minutes was found to be the best with a relative standard deviation (RSD) of 6.8%. In case for 5 minute and 20 minutes, the RSD were found at 45.3 and 11.1 respectively.

4.1.2 Effect of evaporation of MTBE in stirring reactor without catalysts and halogen lamp

A 500 ppb MTBE standard was placed in a stirring reactor in absence of catalysts and halogen lamp to establish the loss of MTBE by evaporation. The samples were collected at 60, 150, and 240 min (1, 1.5, and 4 h) and analyzed using SPME 100 µm PDMS fiber using headspace analysis under GC/MS technique; the results are shown in Figure 14. The results shown below do not support any loss of MTBE under these conditions.

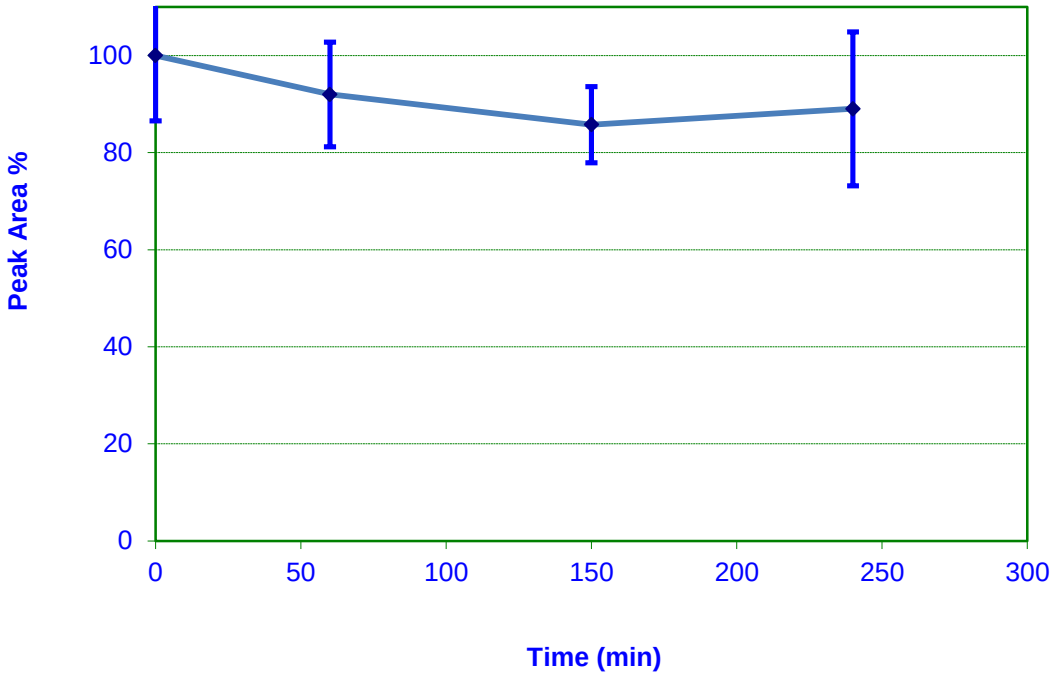

Figure 14. Study of the evaporation effect on MTBE. A 500 ppb MTBE standard was placed in a stirring reactor in absence of catalysts and halogen lamp to establish the loss of MTBE by evaporation. The samples were collected at 60, 150, and 240 min (1, 1.5, and 4 h) and analyzed using SPME 100 µm PDMS fiber using headspace analysis under GC/MS technique. The results showed that the evaporation is not effecting the MTBE degradation.

4.1.3 Degradation of MTBE using halogen lamp and without catalyst in stirring reactor

100 mL of 1000 ppb stock solution of aqueous MTBE was added to the reactor in present of halogen lamp with gentle stirring in absence of any catalyst. Samples were collected at different intervals and analyzed using SPME fiber in conjunction with GC/MS headspace analytical technique. The results are shown in Table 6 and Figure 15. After five hours of continuous stirring, the concentration of MTBE dropped to 42% (peak area %) resulting due to degradation of MTBE in presence of halogen lamp and no catalyst presence.

Table 6. Degradation of MTBE using halogen lamp and without catalyst.

Time	**Peak area response**			**MTBE reduction**
Hour	**Run 1**	**Run 2**	**Average**	**%**
0.00	10521664	10356440	10439052	100.0
0.25	10355906	10032638	10194272	97.7
0.50	9262769	10397688	9830228.5	94.2
1.00	9866627	7683176	8774901.5	84.1
2.00	6490349	7185770	6838059.5	65.5
3.00	6180760	7234747	6707753.5	64.3
4.00	6631420	5288070	5959745	57.1
5.00	4545943	4210910	4378426.5	41.9

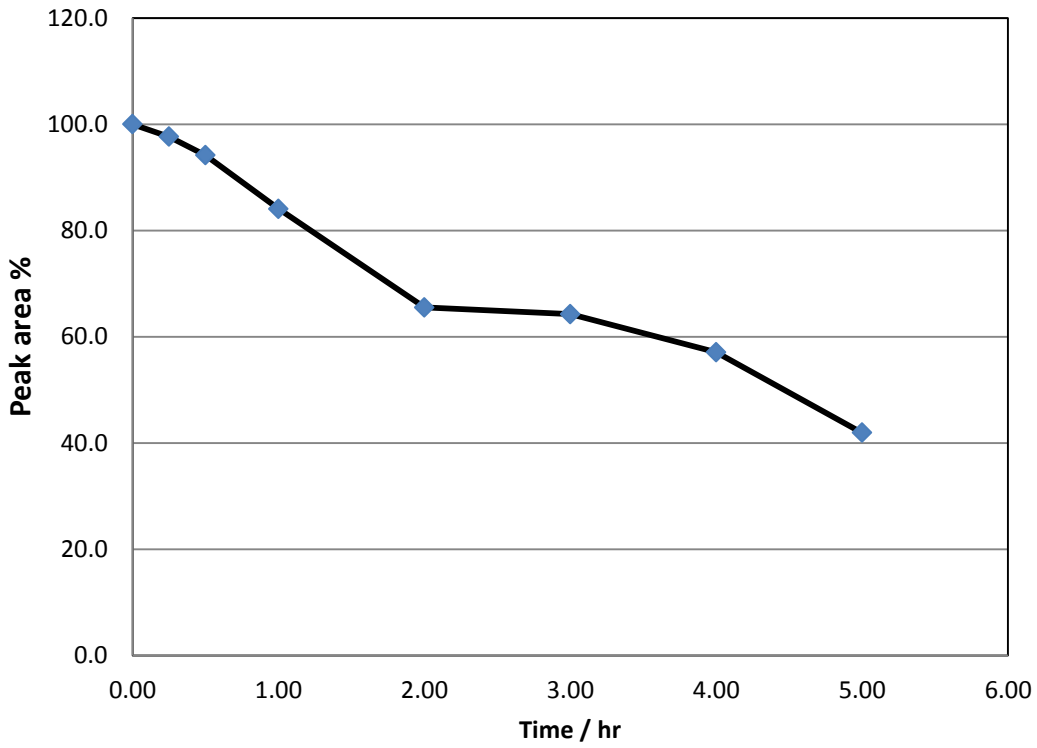

Figure 15. Study of the degradation of MTBE in stirring reactor with halogen lamp and without presence of catalysts. 100 mL of 1000 ppb stock solution of aqueous MTBE was added to the reactor in present of halogen lamp with gentle stirring in absence of any catalyst. Samples were collected at different intervals and analyzed using SPME fiber in conjunction with GC/MS headspace analytical technique. The results are shown in Table 6 and Figure 15. After five hours of continuous stirring, the concentration of MTBE dropped to 42% (peak area %) due to the degradation of MTBE in presence of halogen lamp and in absence of any catalyst.

4.1.4 Degradation of MTBE using halogen lamp and catalyst in stirring reactor

100 mL of 1000 ppb stock solution of MTBE was added to the reactor in present of halogen lamp. A small amount of WO_3 catalyst was added to the solution with gentle stirring. Samples were collected at different intervals and analyzed using SPME fiber in conjunction with GC/MS headspace analytical technique. The results are shown in Table 7 and Figure 16. After five hours of continues stirring under halogen lamp and in presence of catalyst, 74% of MTBE was found to be degraded. It is known that halogen lamp in presence of catalyst (WO_3) has the potential to generate radicals leading to enhanced degradation of MTBE.

Table 7. Degradation of MTBE under halogen lamp and catalyst.

Time	**Peak area response**			**MTBE reduction**
Hour	**Run 1**	**Run 2**	**Average**	**Hour**
0.00	10117754	Not tested	10117754	100.0
0.25	9900683	Not tested	9900683	97.9
0.50	9790270	9595755	9693012.5	95.8
1.00	9090972	8885911	8988441.5	88.8
2.00	6972919	Not tested	6972919	68.9
3.00	4434224	3694216	4064220	40.2
4.00	3836447	3123165	3479806	34.4
5.00	2544145	2738837	2641491	26.1

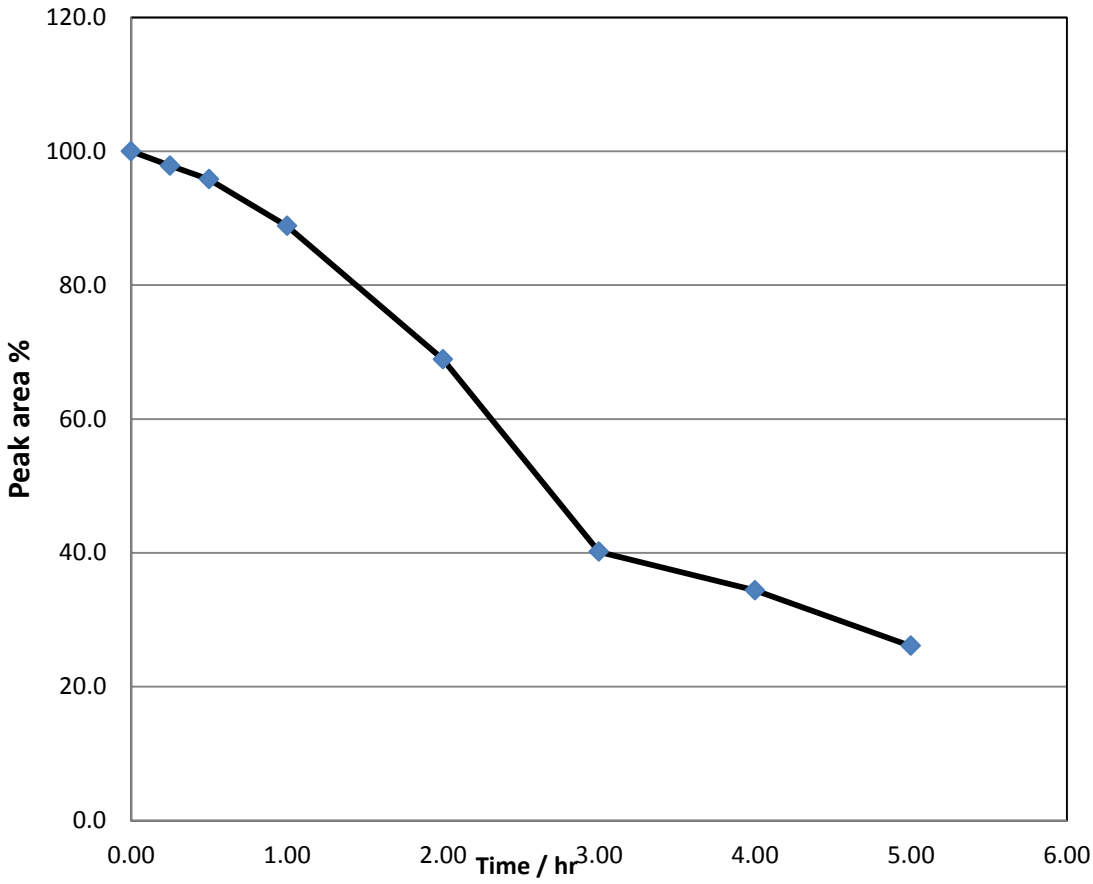

Figure 16. Study the degradation of MTBE in stirring reactor with halogen and catalyst. 100 mL of 1000 ppb stock solution of MTBE was added to the reactor in present of halogen lamp. A small amount of WO_3 catalyst was added to the solution with gentle stirring. Samples were collected at different intervals and analyzed using SPME fiber in conjunction with GC/MS headspace analytical technique. After five hours of continues stirring under halogen lamp and in presence of catalyst, 74% of MTBE was found to be degraded. It is known that halogen lamp in presence of catalyst (WO_3) has the potential to generate radicals leading to enhanced degradation of MTBE.

4.2 Characteristics of noble metals with WO_3

4.2.1 Catalyst Characterization by XRD

The phase identification result of the synthesized WO_3 from sodium tungstate was showed in Figure 17. The XRD result revealed that this catalyst mainly consists of tungsten oxide (WO_3). The phase identification result of the synthesized 1% Pt/WO_3 illustrated in Figure 18. The XRD result confirmed that this catalyst mainly consists of tungsten oxide (WO_3) with minor phase of platinum. In addition, the phase identification result of the synthesized Pt/nano WO_3 was illustrated in Figure 19. The XRD result confirmed that this catalyst mainly consisted of tungsten oxide (WO_3) with the trace phase of platinum.

Furthermore, the phase identification result of the synthesized 2.5% Pt/nano WO_3 was illustrates in Figure 20. XRD result was confirmed that the catalyst mainly consisted of tungsten oxide (WO_3) with the trace of platinum, Figure 21 shows the phase identification result of the synthesized 1% Ru/WO_3, therefore, XRD result revealed that this catalyst mainly consisted of WO_3 with the trace of ruthenium. Figure 22 shows the phase identification result of the synthesized 2% Ru/WO_3. The XRD result revealed that this catalyst mainly consists of tungsten oxide (WO_3) with the trace of ruthenium. In addition, Figure 23 shows the phase identification result of the synthesized 2.5% Ru/nanoWO_3. The XRD result was confirmed that this catalyst mainly consists of tungsten oxide WO_3 with deposition of platinum and ruthenium.

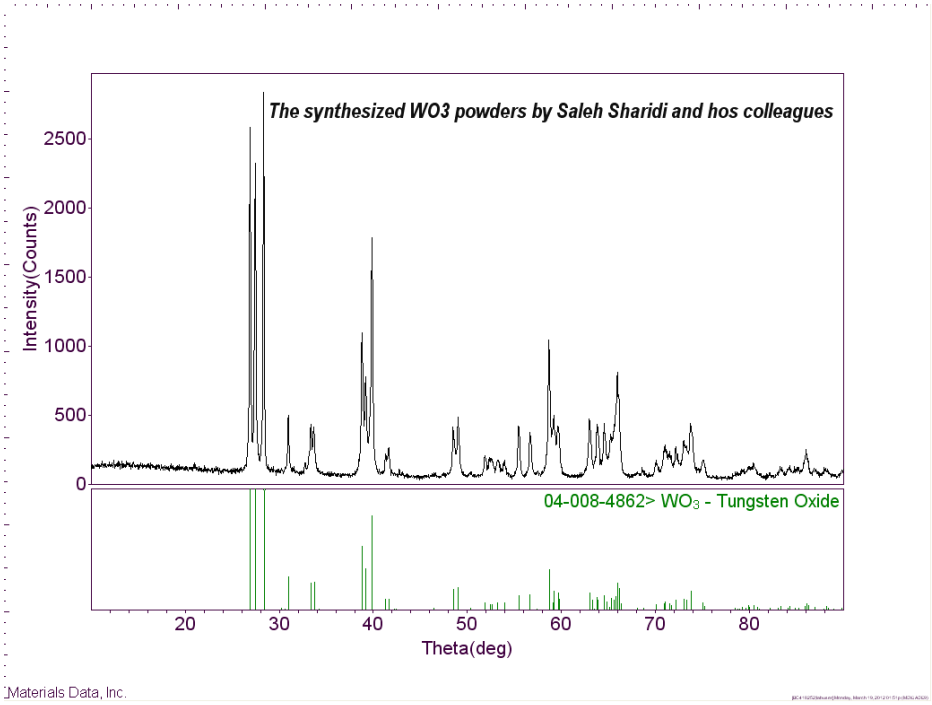

Figure 17. XRD spectrum of synthesized tungsten oxide catalyst. The catalyst was collected with X-ray powder diffractometer with copper X-ray tube (λ=1.54060Å) at ambient conditions along with the identified mineral reference patterns (i.e., ICDD-PDF number 04-008-4862).

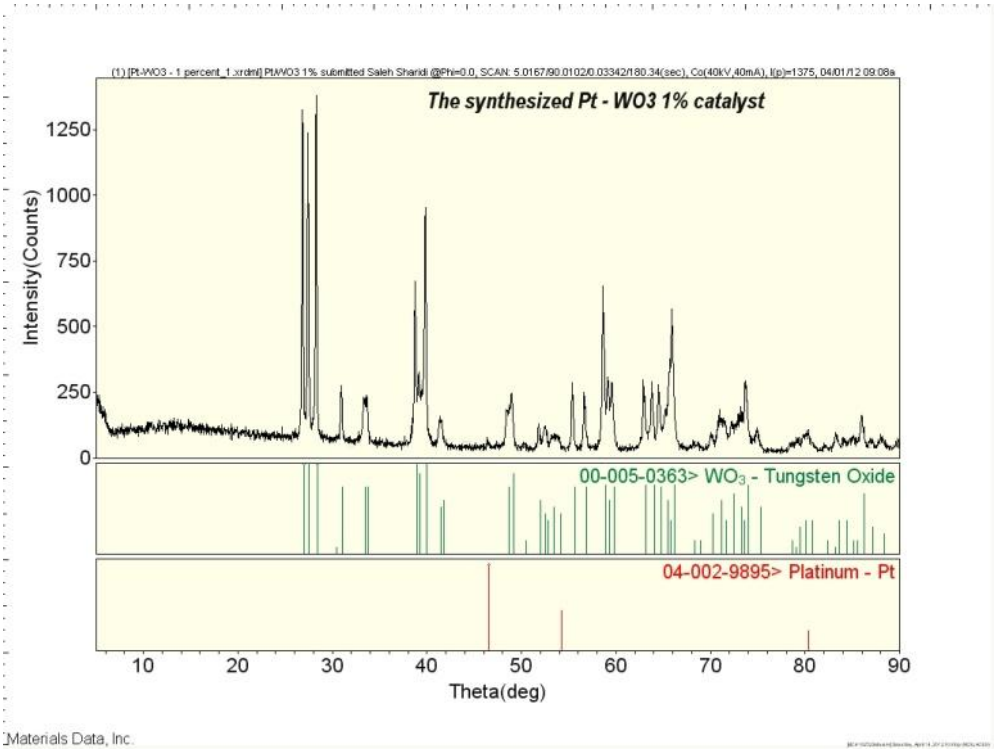

Figure 18. XRD spectrum of synthesized 1% platinum/tungsten oxide catalyst. The catalyst was collected with X-ray powder diffractometer with copper X-ray tube (λ=1.54060Å) at ambient conditions along with the identified mineral reference patterns (i.e., ICDD-PDF numbers 00-005-0363 for WO_3 and 04-002-9895 for Pt

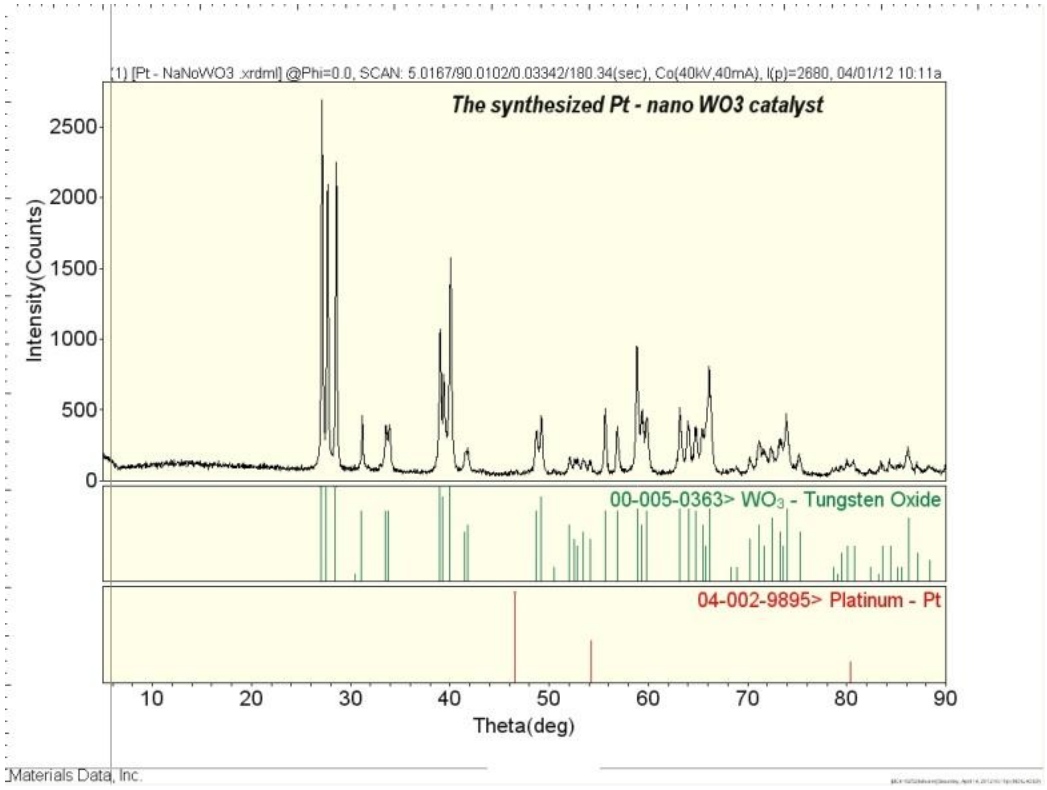

Figure 19. XRD spectrum of the synthesized 1% platinum/nano tungsten oxide. The catalyst was collected with the X-ray powder diffractometer with copper X-ray tube (λ=1.54060Å) at ambient conditions along with the identified mineral reference patterns (i.e., ICDD-PDF numbers 00-005-0363 for WO_3 and 04-002-9895 for Pt).

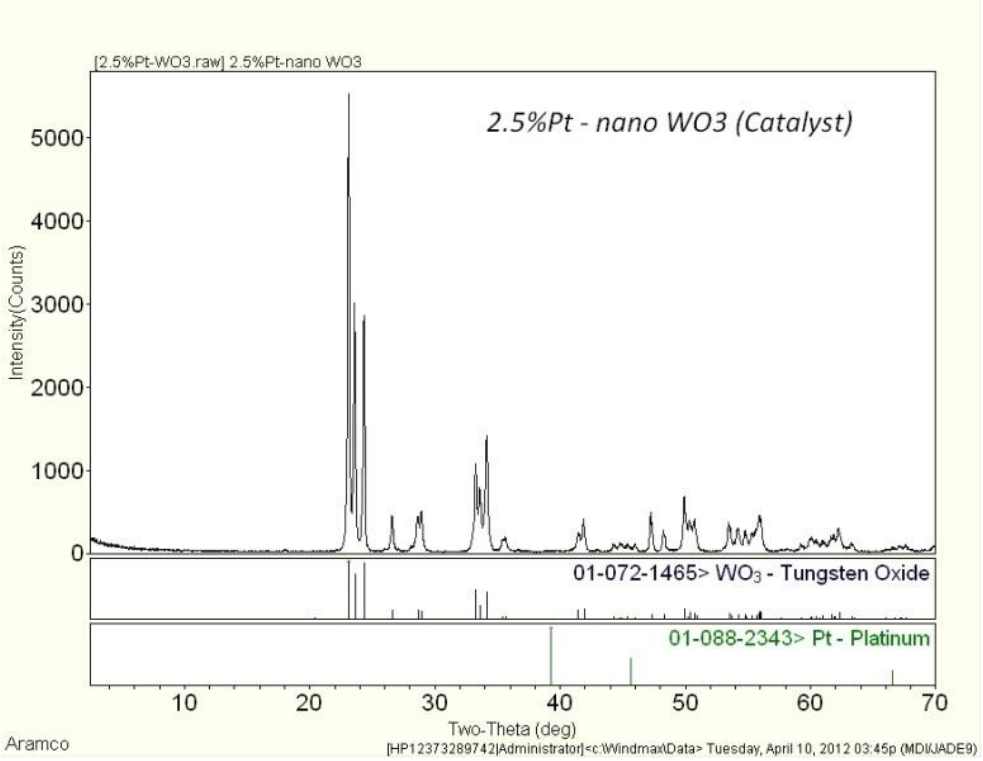

Figure 20. XRD spectrum of synthesized 2.5% platinum/nano-tungsten oxide. The catalyst was collected with X-ray powder diffractometer with copper X-ray tube (λ=1.54060Å) at ambient conditions along with the identified mineral reference patterns (i.e., ICDD-PDF numbers 01-072-1465 for WO_3 and 01-088-2343 for Pt).

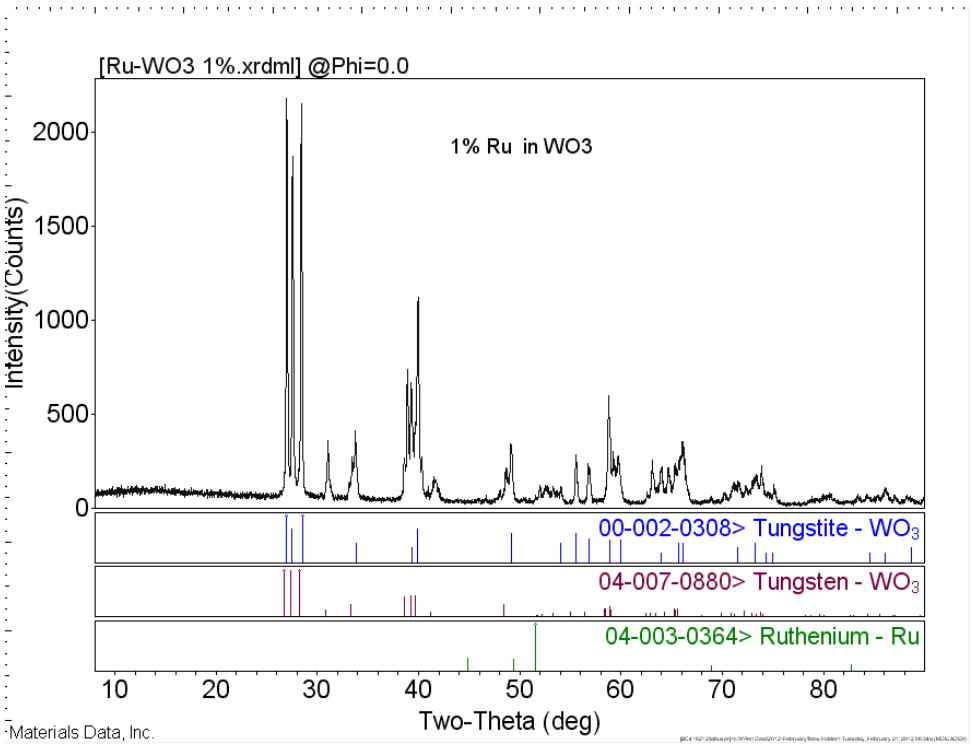

Figure 21. XRD spectrum of synthesized 1% ruthenium/tungsten oxide. The catalyst was collected with X-ray powder diffractometer with copper X-ray tube (λ=1.54060Å) at ambient conditions along with the identified mineral reference patterns (i.e., ICDD-PDF numbers 00-002-0308 and 04-007-0880 for WO_3 and 04-003-0364 for Ru

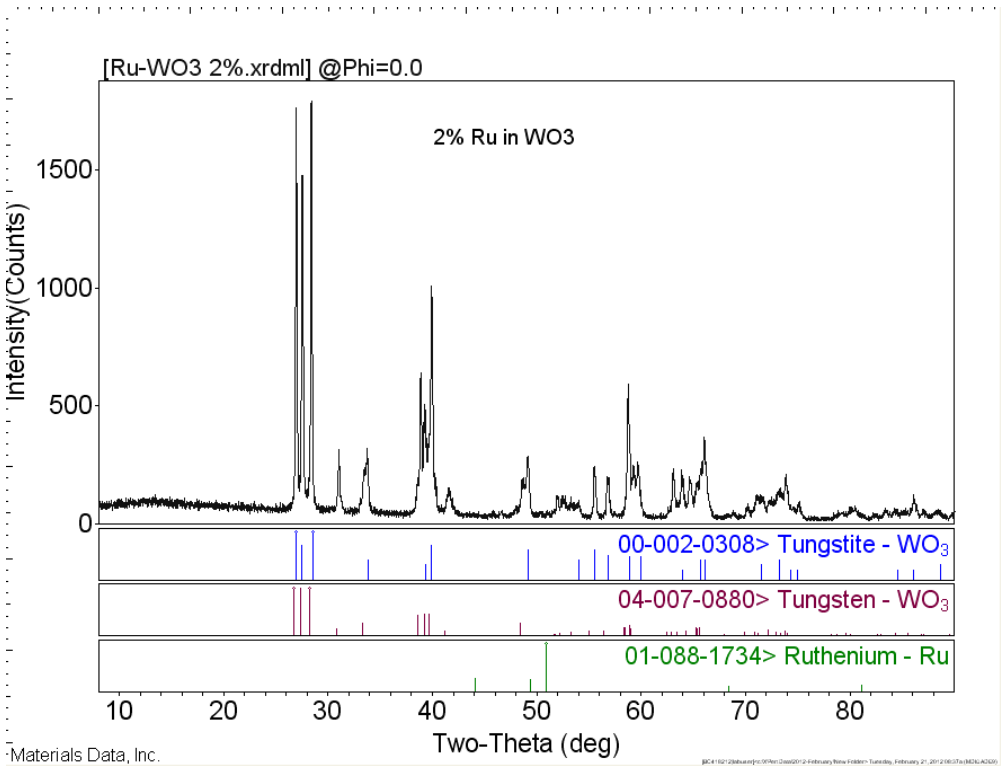

Figure 22. XRD spectrum of synthesized 2% ruthenium/tungsten oxide. The catalyst was collected with X-ray powder diffractometer with copper X-ray tube (λ=1.54060Å) at ambient conditions along with the identified mineral reference patterns (i.e., ICDD-PDF numbers 00-002-0308 and 04-007-0880 for WO_3 and 01-088-1734 for Ru).

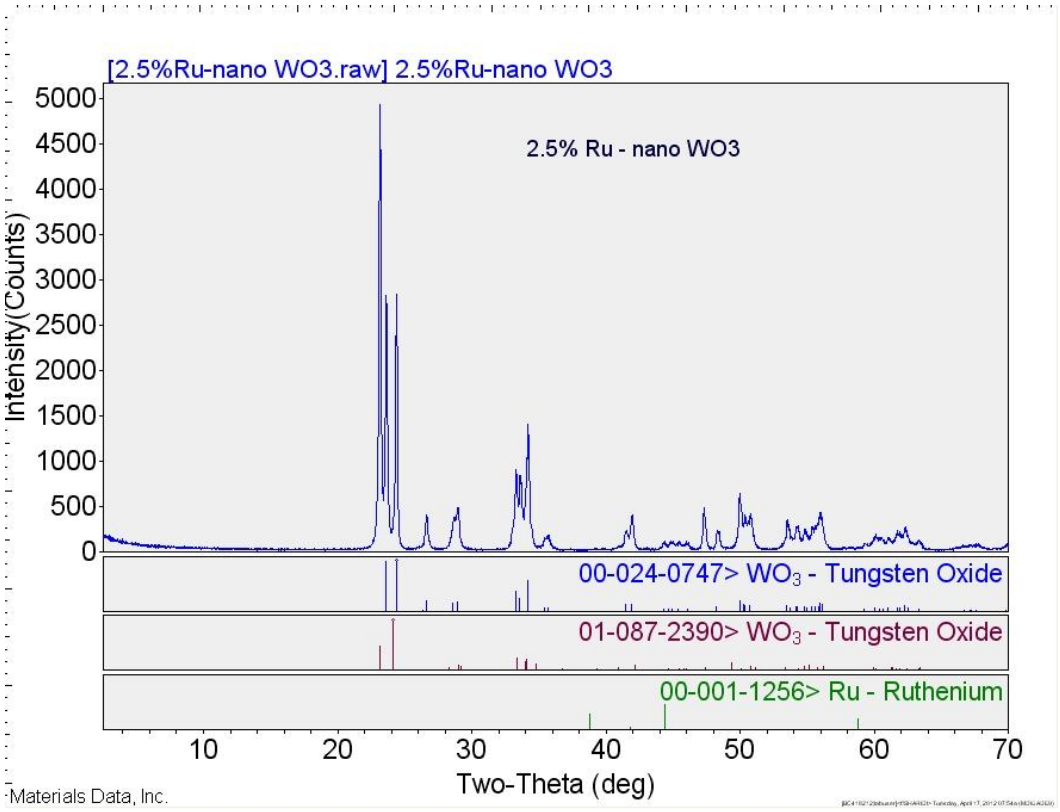

Figure 23. XRD spectrum of synthesized 2.5% ruthenium/nano-tungsten oxide. The catalyst was collected with X-ray powder diffractometer with copper X-ray tube (λ=1.54060Å) at ambient conditions along with the identified mineral reference patterns (i.e., ICDD-PDF numbers 00-024-0747 and 01-087-2390 for WO_3 and 00-001-1256 for Ru).

4.2.2 Environmental Scanning Electron Microscopy (ESEM) Results

The ESEM and EDS analyses were performed using environmental scanning electron microcopy (ESEM) with integrated energy dispersive X-ray spectroscopy system (EDS). The microscope can be operated at voltage up to 30KV in both high vacuum and low vacuum modes and the EDS X-ray detector is ultra-thin window capable of detecting elements down to boron (atomic number 5).The environmental scanning electron microscope has an advantage over the conventional scanning electron microscopy where in the latter coating of non-conductive samples is required to overcome charging problems. In the environmental scanning electron microscope, coating is not required for non-conductive samples, thus preserving the integrity of the samples.

Backscattered and secondary electron images at different magnifications along with EDS X-ray spectra were acquired from the examined samples. The samples were mounted on ESEM stub using double sized conductive carbon tapes and then inserted into the ESEM chamber for examinations. The ESEM and EDS data were acquired using the following operating conditions: 15KV operating voltage, low vacuum mode "0.23Torr", 10mm working distance and spot size 3.

The ESEM surface morphological examination of the original WO_3 showed that this sample consists of regularly shaped fine particles as indicated in Figure 24. As regards the synthesized sample, the ESEM and EDS investigation indicated the formation of platelet-like nano structure of tungsten oxide as shown in Figure 25. Furthermore, ESEM analyses were carried out on Pt/nano WO_3 which showed that the formed product comprises regular shaped nano particles Figure 26, which in agreement with XRD data.

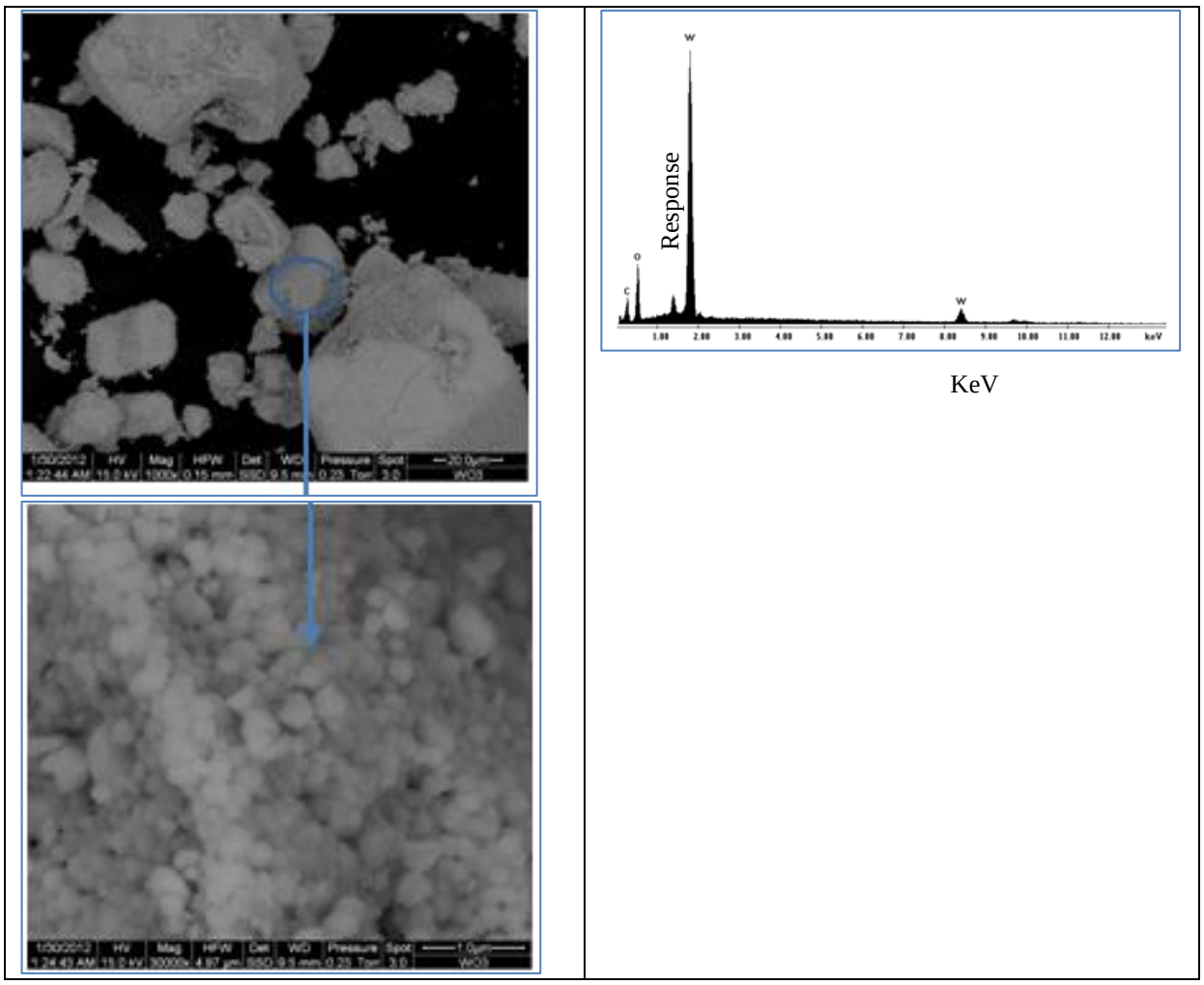

Figure 24. Environmental scanning electron microcopy (ESEM) with integrated energy dispersive X-ray spectroscopy for tungsten oxide. The samples were mounted on ESEM stub using double sized conductive carbon tapes and then inserted into the ESEM chamber for examination. The ESEM and EDS spectra were acquired using following operating conditions: 15KV operating voltage, low vacuum mode "0.23Torr", 10mm working distance and spot size 3. The ESEM surface morphological examination of the original WO_3 showed that this sample consists of regularly shaped fine particles.

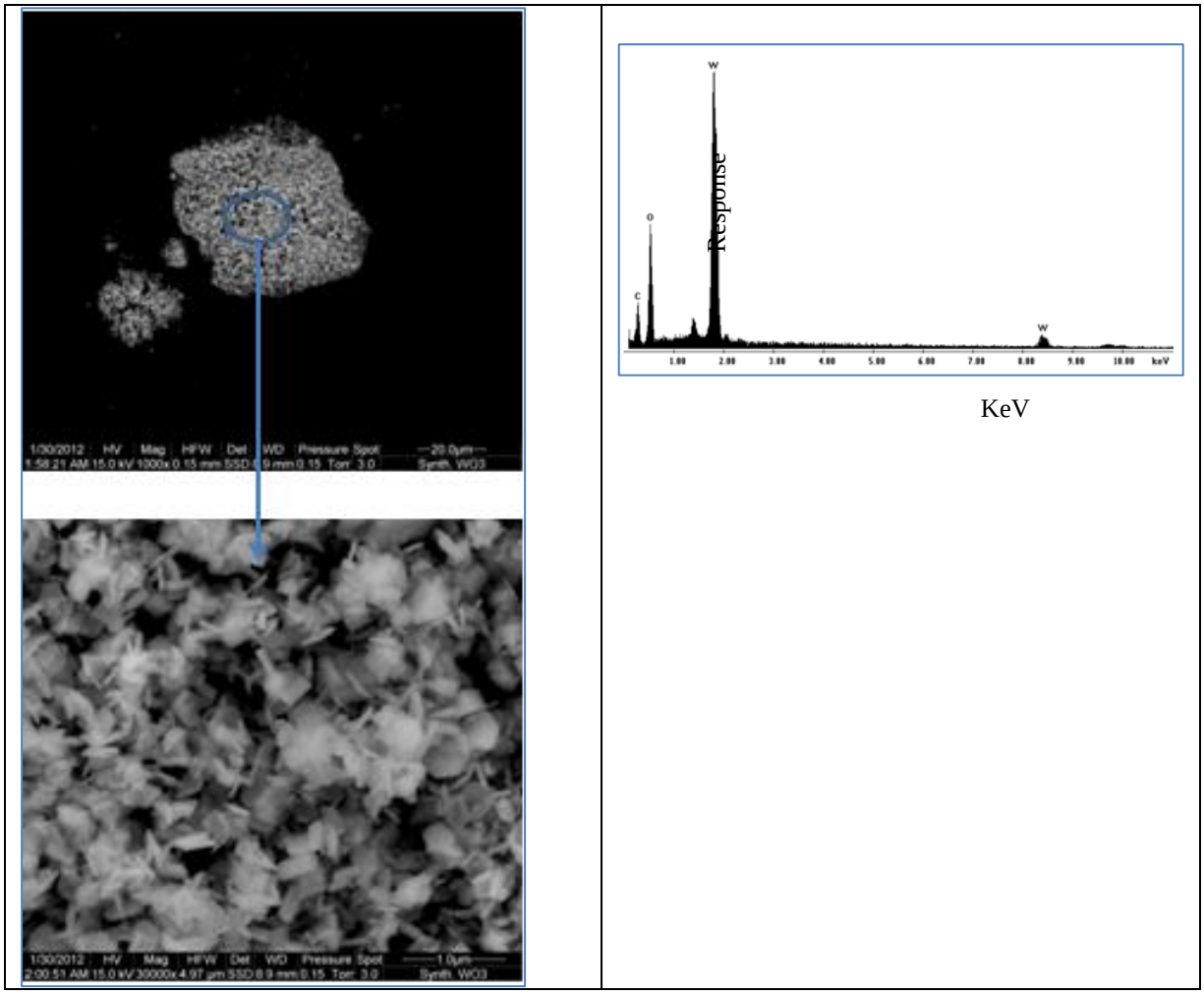

Figure 25. Environmental scanning electron microcopy (ESEM) with integrated energy dispersive X-ray spectroscopy for platelet-like nano structure of tungsten oxide. The samples were mounted on ESEM stub using double sized conductive carbon tapes and then inserted into the ESEM chamber for examinations. The ESEM and EDS spectra were acquired using following operating conditions: 15KV operating voltage, low vacuum mode "0.23Torr", 10mm working distance and spot size 3. The synthesized sample, the ESEM and EDS investigation indicated the formation of platelet-like nano structure of tungsten oxide.

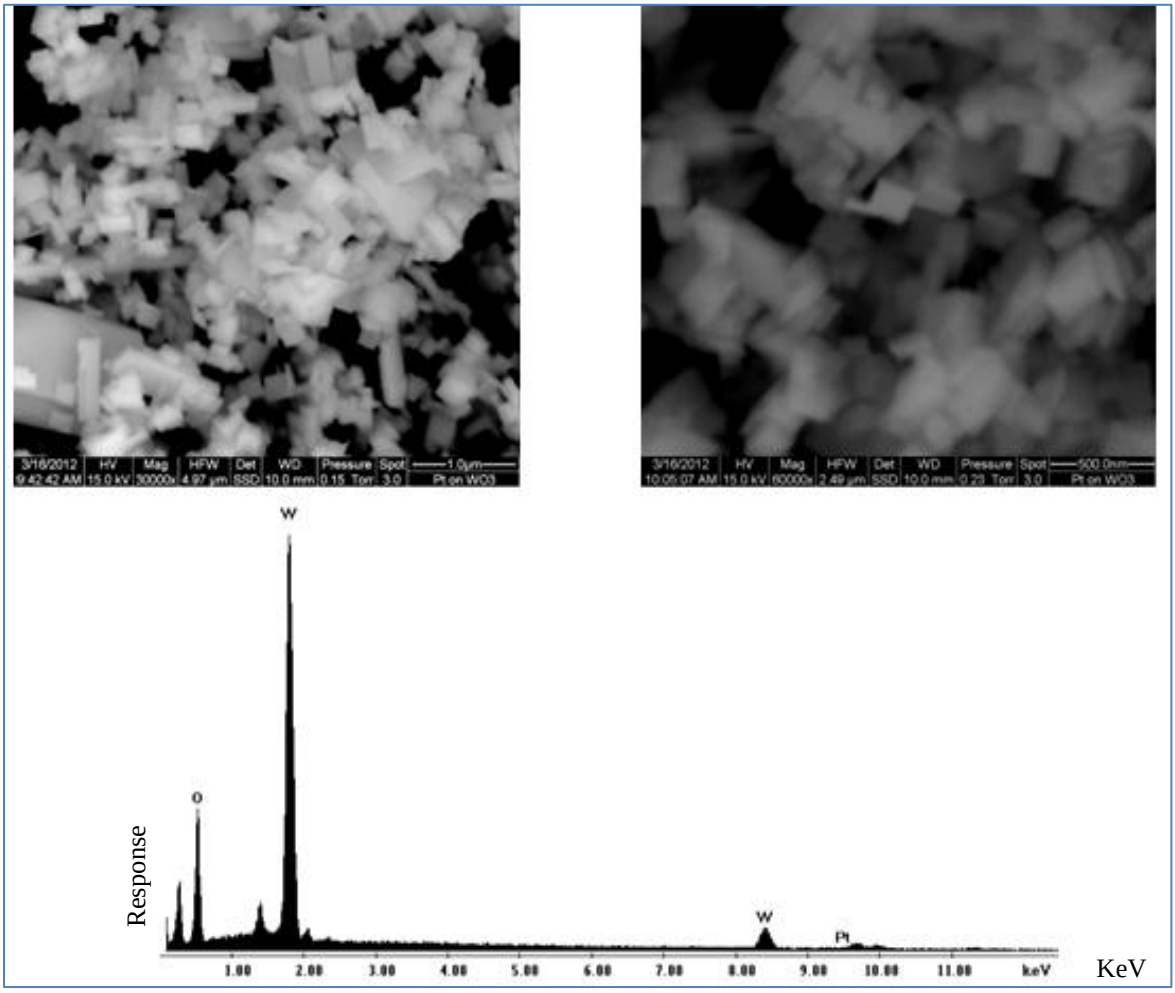

Figure 26. Environmental scanning electron microcopy (ESEM) with integrated energy dispersive X-ray spectroscopy for platinum/nano-tungsten oxide. The samples were mounted on ESEM stub using double sized conductive carbon tapes and then inserted into the ESEM chamber for examinations. The ESEM and EDS spectra were acquired using following operating conditions: 15KV operating voltage, low vacuum mode "0.23Torr", 10mm working distance and spot size 3. ESEM analyses were carried out on Pt/nano WO_3 which showed that the formed product comprises regular shaped nano particles.

4.3 Photocatalytic activity under visible light:

Five active catalysts were prepared and synthesized in the laboratory to establish degradation of MTBE in aqueous solution at presence of visible light. In each case the solution of MTBE was continuously stirred and samples were taken after 4 hours for analysis using SPME headspace GC/MS analysis.

4.3.1 Photooxidation of MTBE via the pure WO_3

The Photooxidation of MTBE was determined by the solid oxide of WO_3 through the halogen lamp excitation for 4 hours of testing. The catalyst was used about 100 mg in 100 ml stock solution contained of 100 ppb MTBE. Table 8 shown the results had a narrow coefficient of variant around ± 0.2-5.9%. The results inducted the reduction of MTBE about 69% after 4 hour, in addition, no hydrocarbon by-product was detected except MTBE reduction as illustrated in Figures 27 and 28 (A-F).

Table 8. Chromatography peak area response of the Photooxidation of MTBE via pure WO_3 catalyst.

	Peak Area (1)	Peak Area (2)	Average Peak Area	RSD %	Aver. Peak Area %
0 hour	1293569	1289281	1291425	0.2	100.00
30 min	1265250	1240041	1252645.5	1.4	97.00
1 hour	925757	818275	872016	5.9	67.52
2 hours	747589	651111	699350	5.3	54.15
3 hours	533264	461878	497571	3.9	38.53
4 hours	415953	377820	396886.5	2.1	30.73

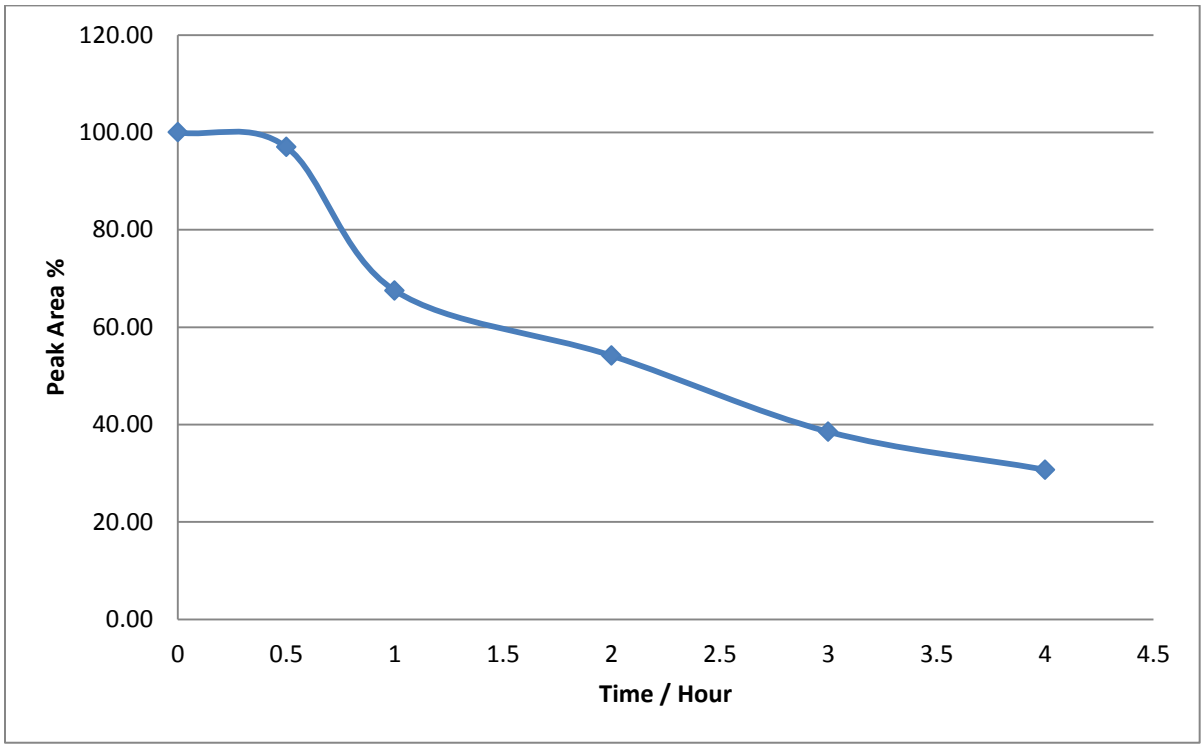

Figure 27. The degradation of MTBE via pure WO_3 using halogen lamp excitation for 4 hours. 100 mg catalyst was added into 100 mL stock solution containing 100 ppb MTBE. A 69% degradation of MTBE took place after 4 hours of treatment with relative standard deviation of ± 0.2-5.9%

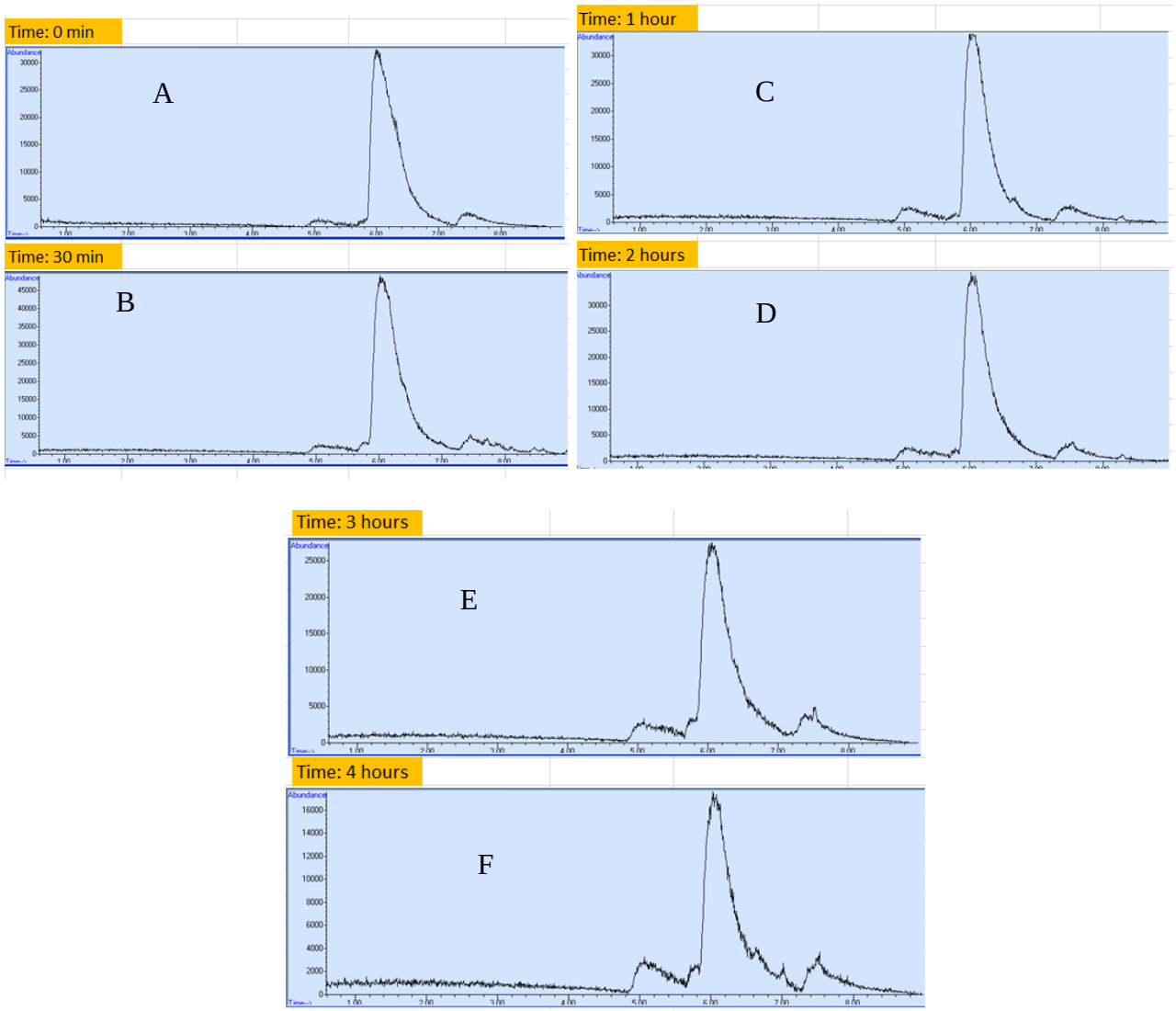

Figure 28 (A-F) illustrated GC-MS chromatography diagram of MTBE treated by pure WO_3 from 0 hour to 4 hours under halogen lamp excitation, catalyst weight 100 mg in 100 mL stock solution contained of 100 ppb MTBE. In addition, the Figures from A to F shows a drop in MTBE peak area but no by-product was detected.

4.3.2 Photooxidation of MTBE by Ru loaded with WO_3

The Photooxidation of MTBE was tested by using different concentration of Ru loaded (0.5, 1.0, 2.0 and 2.5 %) with solid oxide of WO_3. The halogen lamp photooxidation was tested for 4 hours for each catalyst and the weight of each catalyst was 100 mg in 100 ml stock solution contained of 100 ppb MTBE.

Figure 29 (A-D) illustrates the photooxidation result and the chromatography peak area response for each catalysis of 0.5% Ru/WO_3, 1% Ru/WO_3, 2% Ru/WO_3 and 2.5% Ru/WO_3. Figure 30 is shown the Ru/WO_3 degraded the MTBE in one systemically trend and the reduction was ranged from 49 - 79 % of MTBE for 4 hours treatment duration. The results were shown the loading of Ru was not much different reduction of MTBE compared to the pure WO_3. Furthermore, the chromatography of Ru/WO_3 catalysts was shown no hydrocarbon by-products formed.

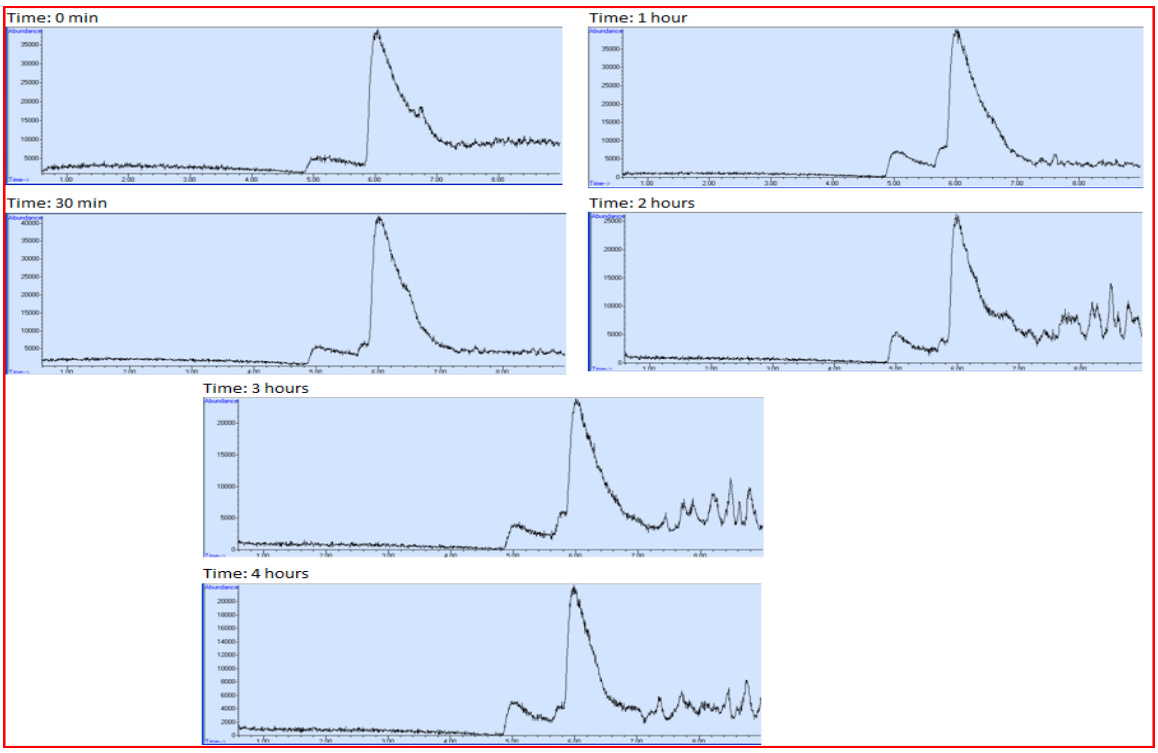

Figure 29 (A) illustrates the GC-MS chromatography diagram of MTBE treated by 0.5% Ru/WO_3, from 0 hour to 4 hours under halogen lamp, catalyst weight 100 mg in 100 mL stock solution contained of 100 ppb MTBE. The figure show degradation of MTBE ranged from 49-79% after 4 hours of treatment. Furthermore, the chromatography of Ru/WO3 catalysts was shown no hydrocarbon by-products formed.

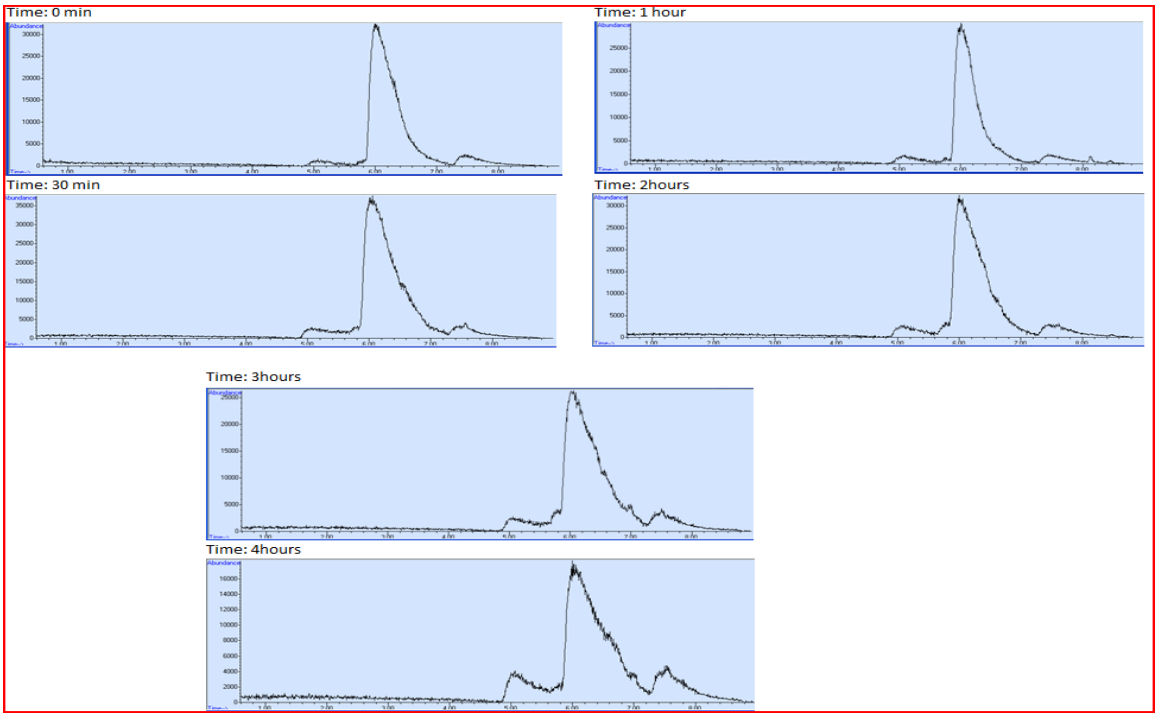

Figure 29 (B) illustrates the GC-MS chromatography diagram of MTBE treated by 1.5% Ru/WO_3, from 0 hour to 4 hours under halogen lamp, catalyst weight 100 mg in 100 mL stock solution contained of 100 ppb MTBE. The figure show degradation of MTBE ranged from 49-79% after 4 hours of treatment. Furthermore, the chromatography of Ru/WO_3 catalysts was shown no hydrocarbon by-products formed.

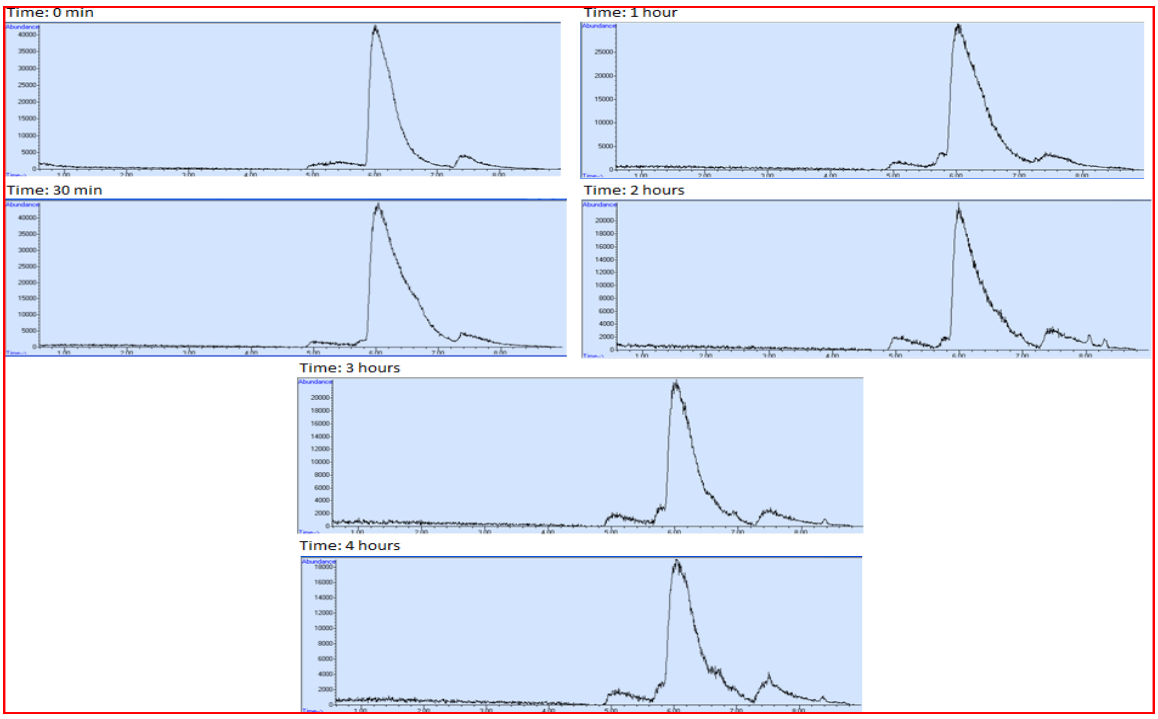

Figure 29 (C) illustrates the GC-MS chromatography diagram of MTBE treated by 2% Ru/WO_3, from 0 hour to 4 hours under halogen lamp, catalyst weight 100 mg in 100 mL stock solution contained of 100 ppb MTBE. The figure show degradation of MTBE ranged from 49-79% after 4 hours of treatment. Furthermore, the chromatography of Ru/WO3 catalysts was shown no hydrocarbon by-products formed.

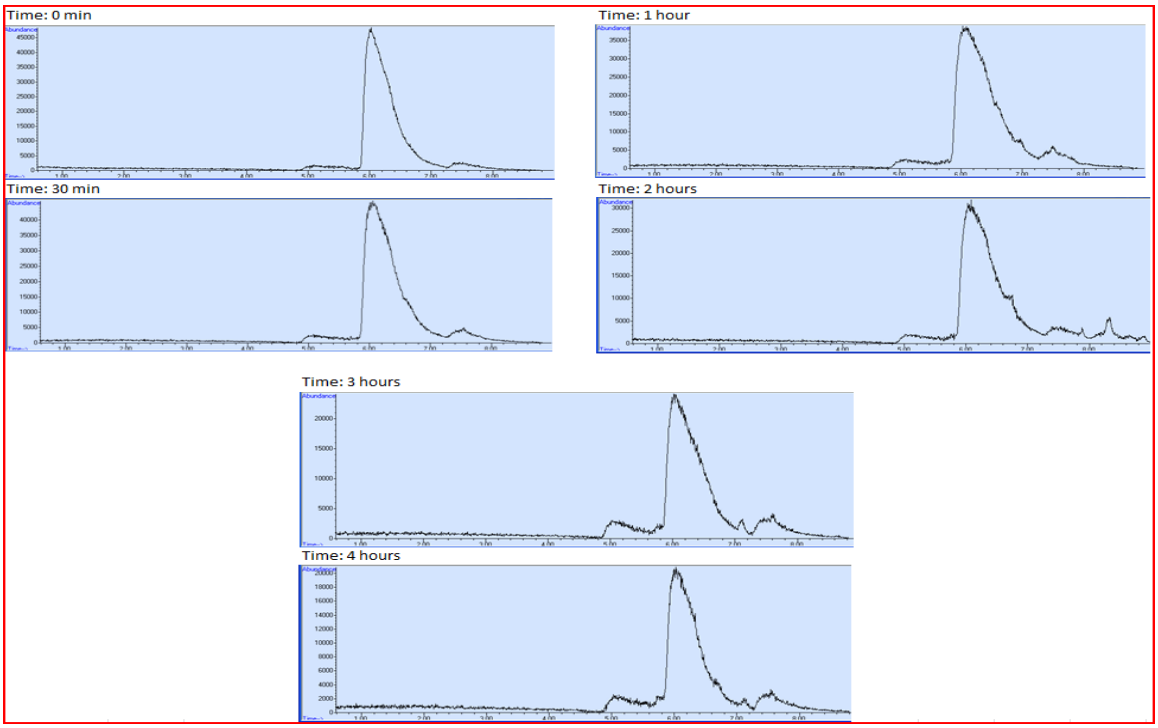

Figure 29 (D) illustrates the GC-MS chromatography diagram of MTBE treated by 2.5% Ru/WO_3, from 0 hour to 4 hours under halogen lamp, catalyst weight 100 mg in 100 mL stock solution contained of 100 ppb MTBE. The figure show degradation of MTBE ranged from 49-79% after 4 hours of treatment. Furthermore, the chromatography of Ru/WO_3 catalysts was shown no hydrocarbon by-products formed.

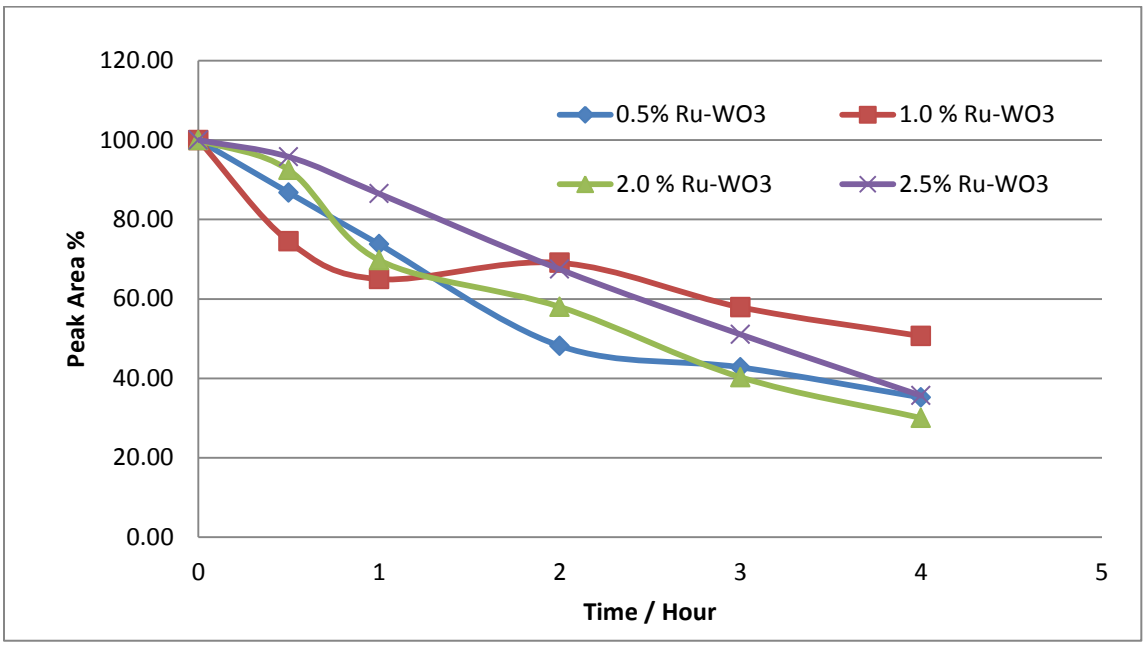

Figure 30. The degradation of MTBE via different concentration (0.5%, 1.0%, 2.0% and 2.5%) of Ru loaded on WO_3 treated by halogen lamp and catalyst weight 100 mg in 100 mL stock solution contained of 100 ppb MTBE. The Ru/WO_3 degraded the MTBE in one systemically trend and the reduction was ranged from 49 - 79 % of MTBE for 4 hours treatment. The results show that the loading of Ru was not much different for reduction of MTBE compared to the pure WO_3.

4.3.3 Photooxidation of MTBE by Ru loaded on nanoWO_3

The Photooxidation of MTBE was tested by using nano solid oxide of WO_3 by using different concentration of Ru loaded (0.5, 1.5 and 2.5 %). The photooxidation was tested for 4 hours for each catalyst and the weight of each catalyst was 100 mg in 100 ml stock solution contained of 100 ppb MTBE.

Figure 31 (E-G) illustrates the photooxidation result and the chromatography peak area response for each nano WO_3 catalysis loaded by 0.5% Ru/nanoWO_3, 1.5% Ru/nanoWO_3 and 2.5% Ru/nanoWO_3. Figure 32 is shown the nano WO_3 loaded by Ru catalyst were degraded the MTBE in one systemically trend and the reduction was ranged from 39 - 62 % of MTBE for 4 hours treatment duration. The results indicted increase of Ru, lead to decrease the activity of WO_3 and no increase of the MTBE reduction. In addition, GC-MS chromatography at Figure 31 (E-G) was shown no hydrocarbon by-products detected.

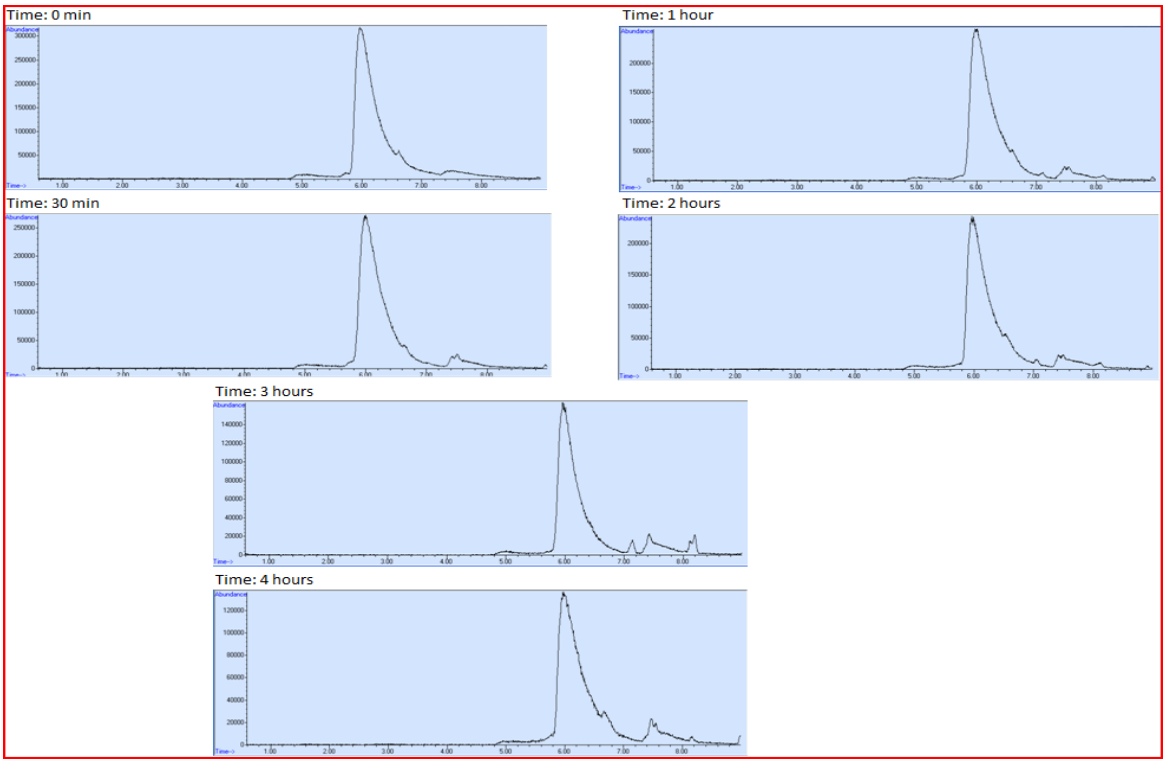

Figure 31 (E) Illustrated GC-MS chromatography diagram of MTBE treated by 0.5% Ru/nano WO_3 from 0 hour to 4 hours under halogen lamp, catalyst weight 100 mg in 100 mL stock solution contained of 100 ppb MTBE. The figure show small degradation of MTBE and shown no hydrocarbon by-products.

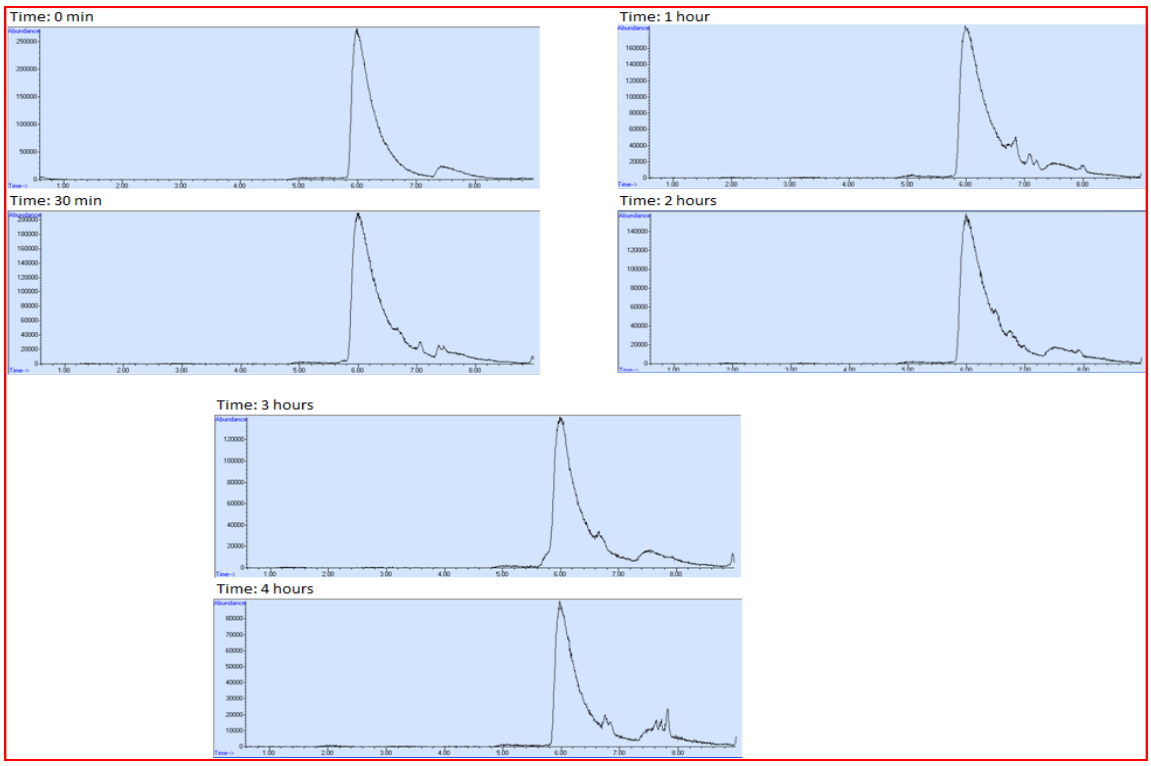

Figure 31 (F) Illustrated GC-MS chromatography diagram of MTBE treated by 1.5% Ru/nano WO_3 from 0 hour to 4 hours under halogen lamp, catalyst weight 100 mg in 100 mL stock solution contained of 100 ppb MTBE. The figure show no degradation of MTBE and shown no hydrocarbon by-products.

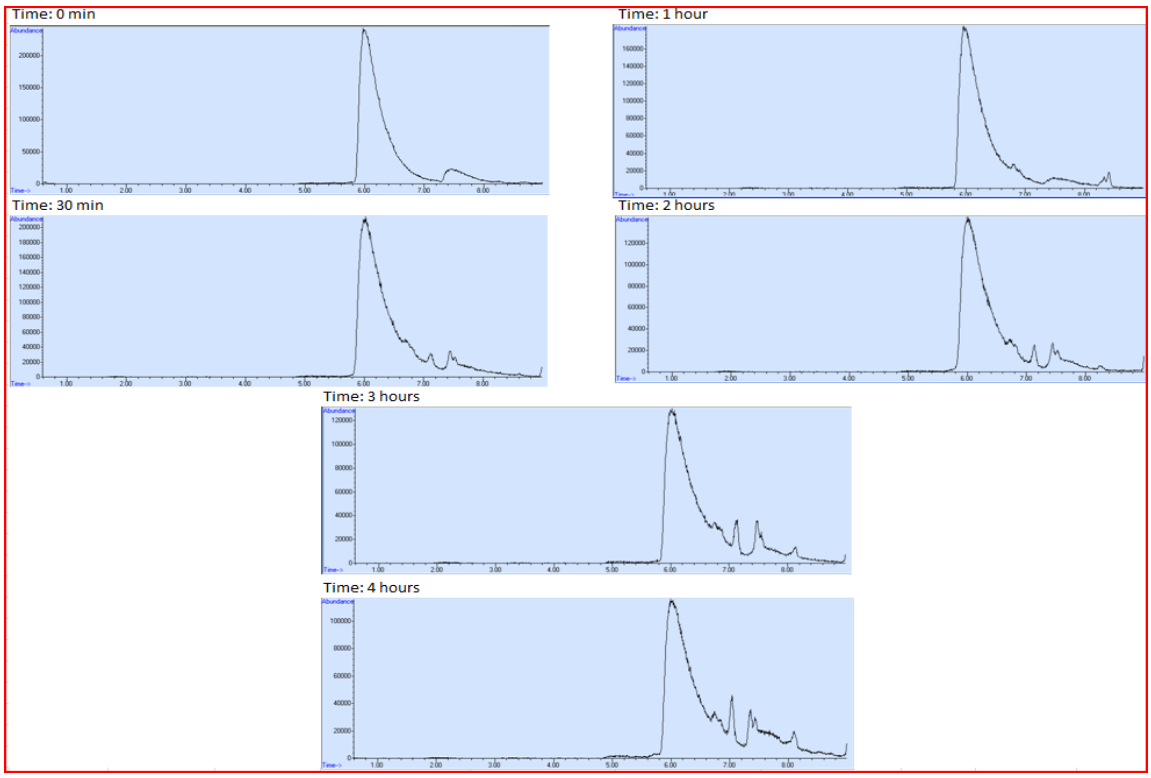

Figure 31 (G) Illustrated GC-MS chromatography diagram of MTBE treated by 2.5% Ru/nano WO_3 from 0 hour to 4 hours under halogen lamp, catalyst weight 100 mg in 100 mL stock solution contained of 100 ppb MTBE. The figure show no degradation of MTBE and shown no hydrocarbon by-products.

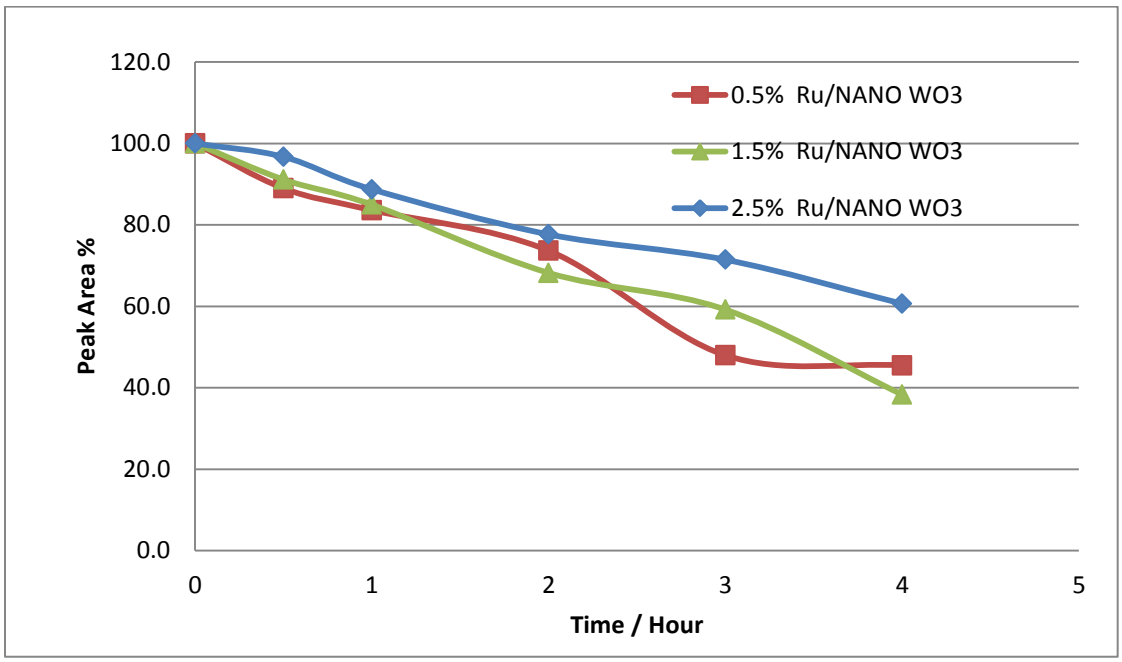

Figure 32. The degradation of MTBE via different concentration (0.5%, 1.5% and 2.5%) of Ru loaded on nano WO_3 treated by halogen lamp and catalyst weight 100 mg in 100 mL stock solution contained of 100 ppb MTBE. The degradation ranged from 39 - 62 % of MTBE for 4 hours treatment. The results indicted increase of Ru, lead to a drop in the activity of WO_3 but no increase in the degradation of MTBE.

4.3.4 Photooxidation of MTBE via Pt loaded on WO_3

The Photooxidation of MTBE was tested by using five different concentration of Pt loaded in WO_3 were 0.5, 1.0, 1.5, 2.0 and 2.5 %. The photooxidation was tested for 4 hours for each catalyst and the weight of each catalyst was 100 mg in 100 mL stock solution contained of 100 ppb MTBE.

Figure 33 showed the Pt loaded on WO_3 were degraded the MTBE steeply and increased after 1 to 3 hours; in addition, after 4 hours the MTBE treatment achieved 98%.

Figure 34 (A-F), the GC-MS chromatography diagram illustrates the photooxidation of 0.5% Pt/WO_3 to MTBE, after 1 hour the by-product of formic acid 1,1-dimethylethyl ester was generated during the oxidation. The by-product was increased as MTBE decreased after 2 hours of the treatment. Then, at 3 hours the MTBE reduced more than 90% and the by-product started to decrease as well. The observation of the by-product after 4 hours treatment was decreased to trace level.

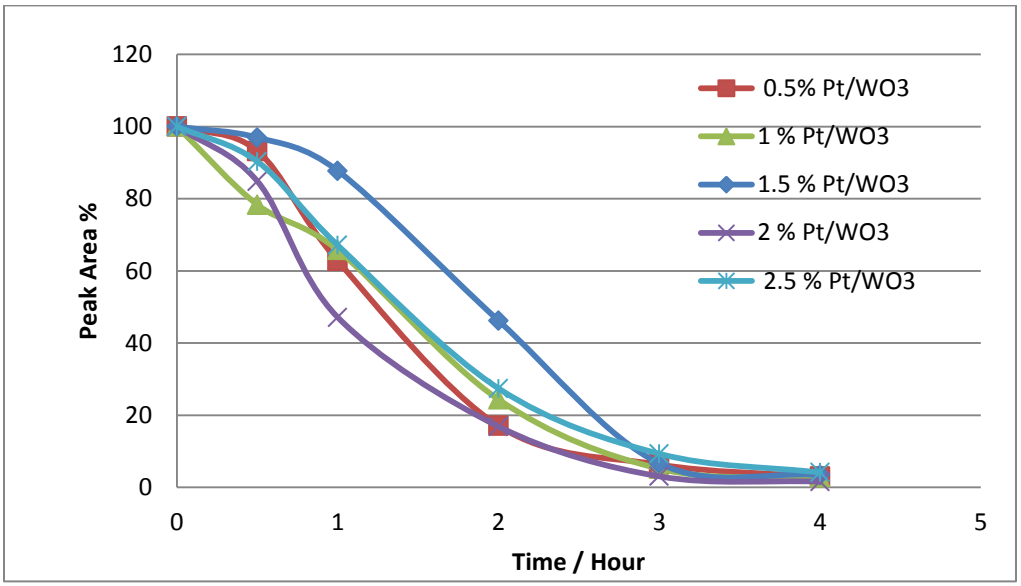

Figure 33. The degradation of MTBE via different concentration of Pt loaded on WO_3 and treated by halogen lamp, 100 mg catalyst in 100 mL stock solution containing 100 ppb MTBE. The degradation of MTBE was very steep and degradation intensified after 1 to 3 hours. After 4 hours 98% MTBE degradation was achieved.

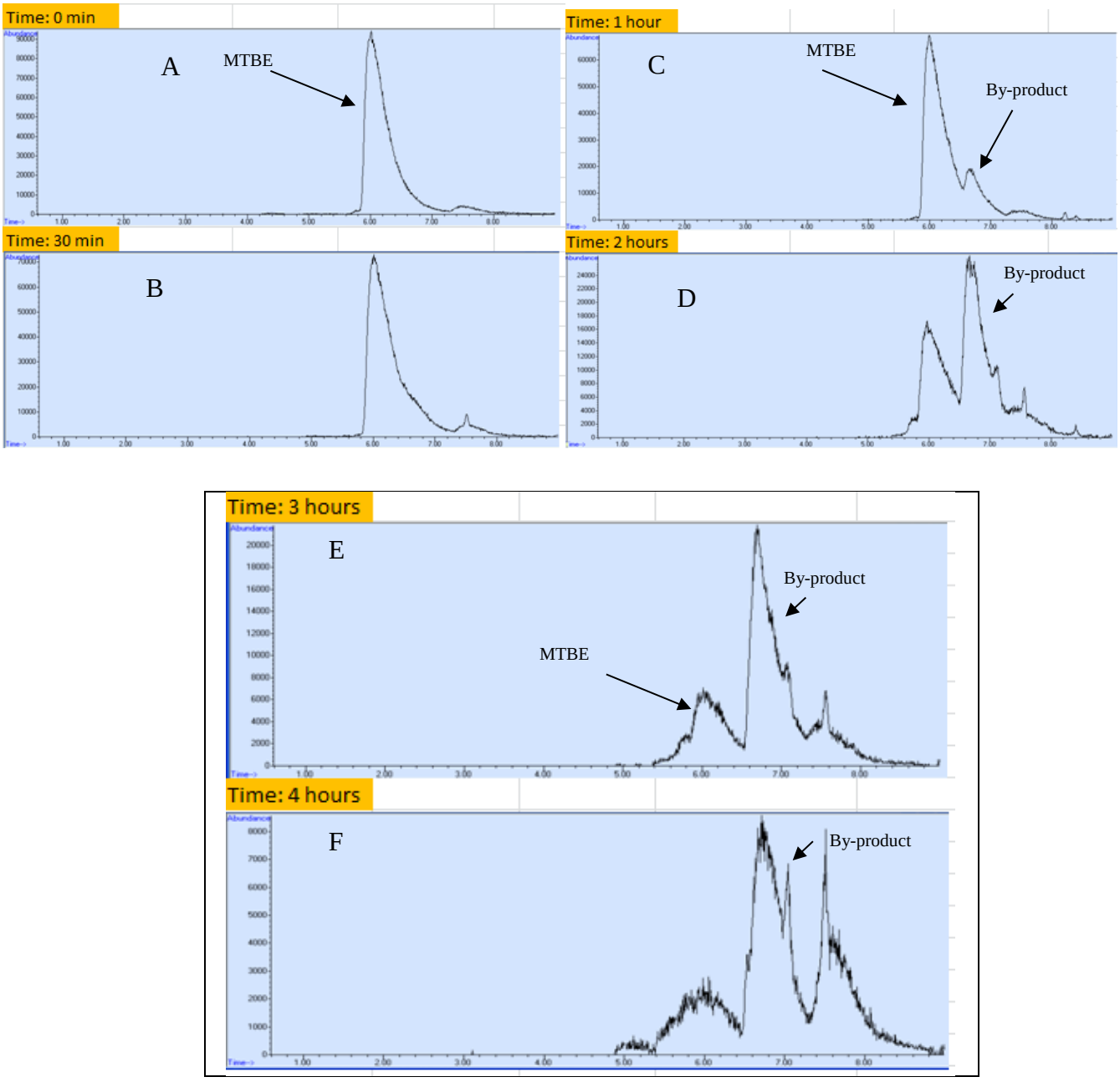

Figure 34 (A-F) Illustrated GC-MS chromatography diagram of MTBE treated by 0.5% Pt/WO_3 from 0 hour to 4 hours under halogen lamp, catalyst weight 100 mg in 100 mL stock solution containing 100 ppb MTBE.

4.3.5 Photooxidation of MTBE by Pt in nanoWO_3

The nano WO_3 loaded by Pt for ratio of 0.5, 1.5 and 2.5% and tested through photooxidation of MTBE. The experiment was performed 4 hours treatment duration for each catalyst and the weight of each catalyst was 100 mg in 100 mL stock solution contained of 100 ppb MTBE.

Figure 35 illustrated the photooxidation results of 0.5% Pt/nano WO_3. The GC-MS chromatography was shown dramatically decrease of MTBE molecule after 0.5 hour of the photooxidation treatment and by-product of MTBE produced formic acid 1, 1-dimethylethyl ester form the treatment. Figure 36 was shown the Pt loaded on nano WO_3 achieved MTBE degradation more than 85% after 1 hour of the treatment. In addition, the three loaded percentage of Pt in nano WO_3 were achieved 99% of MTBE degradation after 3 hours of the treatment with trace of by-product. Nevertheless, the by-product was effectively reduced from the sample after 3 hours at Pt/nano WO_3 compared to the photooxidation of Pt/WO_3 treatment.

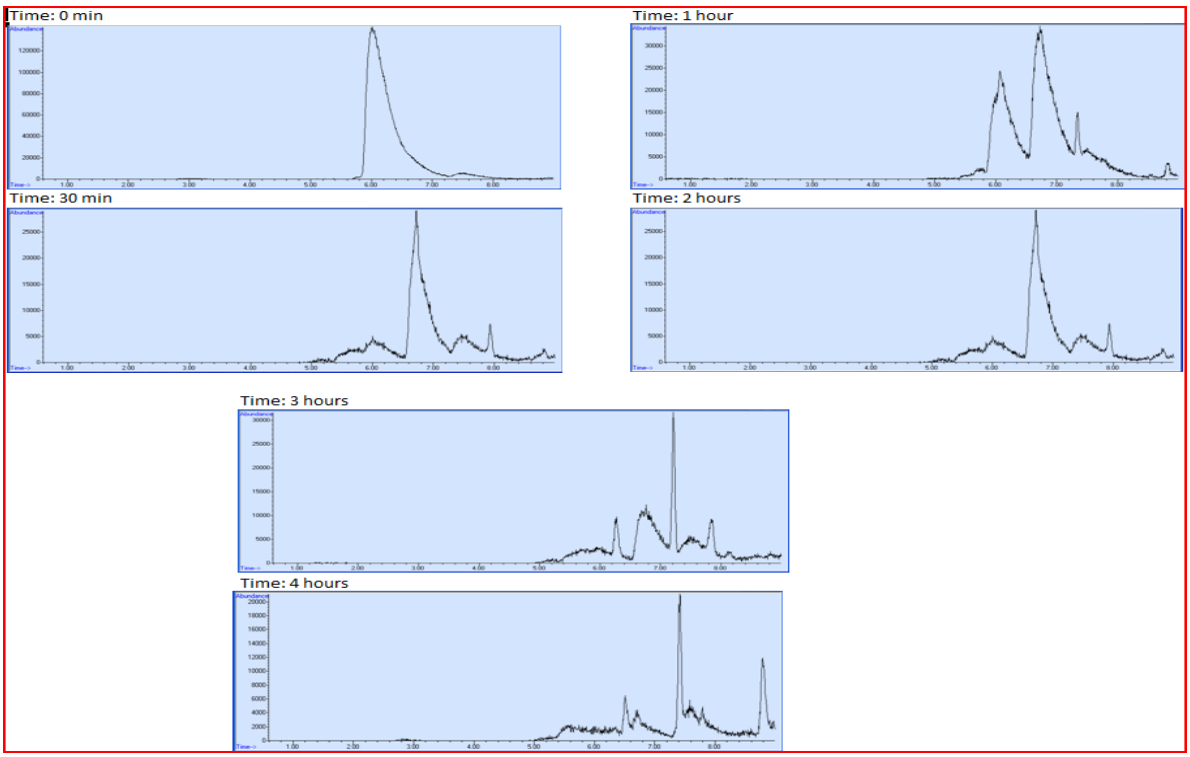

Figure 35. illustrated the photooxidation result and the GC-MS chromatography diagram for 0.5% concentration of Pt catalyst loaded on nano WO_3. The GC-MS chromatography was shown the MTBE peak at 90,000 peaks high. After 1 hour of photooxidation treatment, the MTBE molecule started to decrease and by-product of MTBE produced formic acid 1, 1-dimethylethyl ester form the treatment. After 2 hours, the MTBE decreases and by products increases at 24, 000 peaks high and increase up to 29,000 peaks high. After 3 hours of treatment, MTBE decrease and by product started to decrease to trace amount.

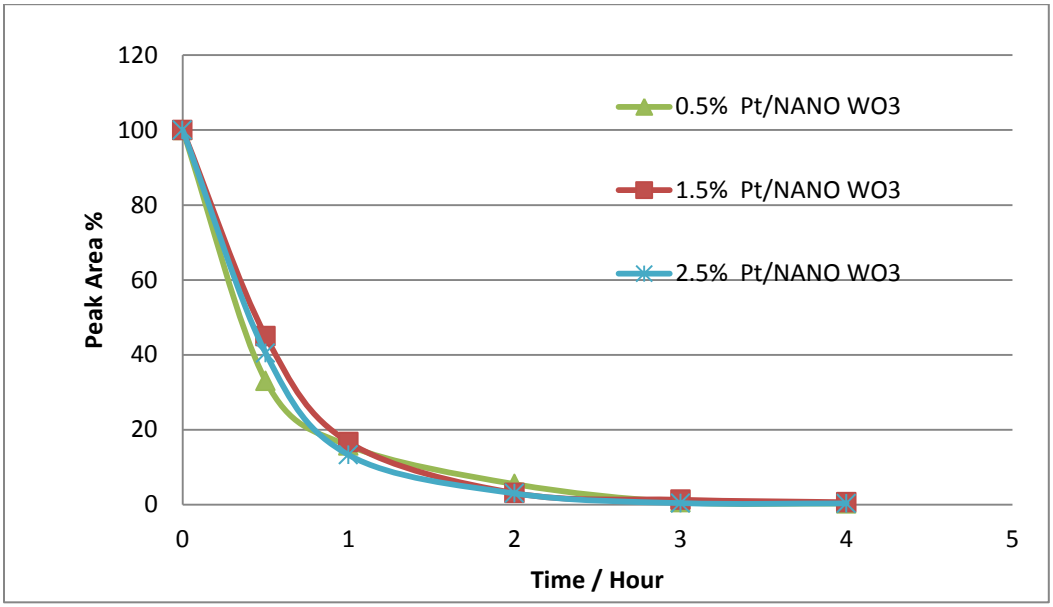

Figure 36. The degradation of MTBE via different concentration of Pt loaded on nano WO_3 treated by halogen lamp with catalyst weighing 100 mg in 100 mL stock solution of 100 ppb MTBE. After three hours of treatment around 99% degradation MTBE was achieved.

4.3.6 By-product of vis.light photooxidation by Pt/nano WO_3

The by-product from the photooxidation via catalyst of Pt/WO3 was observed. The GC-MS library was applied by using NIST 2007 database in order to determine the by-product generated during the photooxidation of MTBE reduction. The mass ion of formic acid $1,1-$ dimethylethyl ester was determined by the mass fragmentation of GC-MS and it has known by m/z 87, m/z 59 and m/z 57 from the MS database matching percentage of 64%. After one hour photooxidation treatment, the by-product concentration increased during the treatment with mass ion matching percentage increased to 77%; in addition, that could confirm the singlet oxygen might introduced to MTBE compound and the retention time was moved slightly as shown in Figure 37.

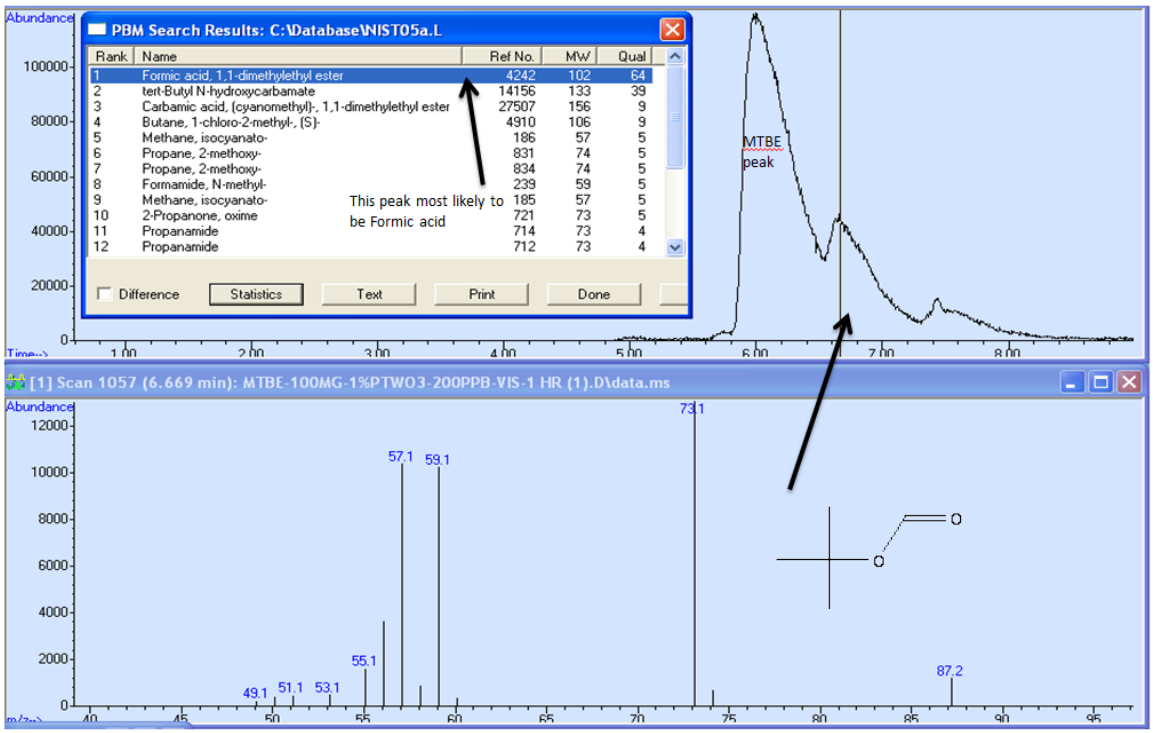

Figure 37. NIST 2007 database of formic acid 1,1 – dimethylethyl ester after 1 hour degradation. In addition, the mass fragmentation of molecule was identified by m/z 87, m/z 59 and 57 from database of MS.

4.4 Conclusions

The research supports the degradation of visible light photooxidation to MTBE through selected catalysts. The Pt/WO_3 and $Pt/nanoWO_3$ has demonstrated the pathway of MTBE degradation to formic acid 1,1-dimethylethyl ester. The photooxidation by vis light was performed almost complete degradation of MTBE to CO_2 and H_2O with trace of by-products.

In addition, the study has also demonstrated the photooxidation of MTBE by using pure WO_3, Ru/WO_3 and Ru/nano WO_3; however none of these combinations get to 99% degradation of MTBE.

4.5 References

[1] Azadeh. A and Mehrab. M Degradation of aqueous Methyl tert-Butyl Ether by photochemical, biological, and their combined processes. International Journal of Photoenergy. Volume, Article ID 19790, pp 1–7 (2006).

[2] Azadeh, A and Mehrab M., Degradation of Aqueous Methyl tert-Butyl Ether by Photochemical, Biological, and Their Combined Processes, International Journal of Photoenergy, Article ID 19790, Pages 1–7, Volume 2006.

[3] Barreto, R, Gray, K. Anders, K. Photocatalytic degradation of methyl-tert-butyl ether in TiO2 slurries: a proposed reaction scheme. Water Research , 29 (5), 1243-8 (1995).

[4] Burbank A., Dionysiou D., Suidan M., and Richardson T., Oxidation kinetics and effect of pH on the degradation of MTBE with Fenton Reagent. Water research, vol. 39, no1, pp. 107-118 2005.

[5] Buscheck. Occurrence and Behavior of MTBE in Groundwater. Underground Storage Tank Conference, Los Angeles, State of California Water Resources Control, Sacramento (1998).

[6] Melin, G: Treatment Technologies for Removal of Methyl Tertiary Butyl Ether (MTBE) from Drinking Water, (Ed. 2), National Water Research Institute, Fountain Valley, CA. California USA, 2000.

[7] Davidson, J. and Creek D.: Granular Activated Carbon, in Treatment Technologies for Removal of Methyl Tertiary Butyl Ether (MTBE) From Drinking Water: Air Stripping, Advanced Oxidation Processes (AOP), and Granular Activated Carbon (GAC). Fort Collins, CO: Alpine Environmental, prepared for MTBE Research Partnership. DC., 1998.

[8] Dale, M., Moylan, B., and Davis M.: MTBE Taste and Odor Threshold Determinations Using the Flavor Profile Method. Metropolitan Water District of Southern California, 1997.

[9] Delzer, G., Grady, J., Zogorski, B., Rowe, L. and Koch, B.: National Survey of MTBE, Other Oxygenates, and Other VOCs in Community Drinking-Water Sources, 2001.

[10] Gullick, R., and LeChevallie, M.: Occurrence of MTBE in drinking water sources. Jour. AWWA, v. 92, n. 1, pp. 100-113, 2000.

[11] Happel, A., Beckenbach, E and Halden R.: An Evaluation of MTBE Impacts to California Groundwater. Lawrence Livermore National Laboratory, Livermore, CA UCRLAR- 130897, 1998.

[12] INCHEM. International Programme on Chemical Safety, Environmental Health Criteria206, MTBE, 1998

[13] Jia, L., Fang X, Deju, W., Jue, H. and Weimin, C.: The application of silicalite-1/fly ash cenosphere (S/FAC) zeolite composite for the adsorption of methyl tert-butyl ether (MTBE), Journal of Hazardous Materials, Volume 165, Issues 1-3, 15, Pages 120-125, June 2009.

[14] Araña, A., Peña Alonso, J., Doña R., Herrera M., González, D. and Pérez, P.: Comparative study of MTBE photo catalytic degradation with TiO_2 and Cu-TiO_2 , Applied Catalysis B: Environmental, Volume 78, Issues 3-4, 7, pages 355-363, February 2008.

[15] Kang, J., and M.R. Hoffmann, M.: Kinetics and mechanism of the sonolytic destruction of mtbe by ultrasonic irradiation in the presence of ozone. Jour. Environmental Science and Technology, v. 32, N. 20, PP. 3194-3199, 1998.

[16] Mezyk, S., Cooper, D., Bartels, K., and Wu, T.: Radiation chemistry of alternative fuel oxygenates: substituted ethers. J. Phys. Chem. Part A, v. 105, pp. 3521-3526, 2001.

[17] Stefan, M., Mack, J, and Bolton, J: Degradation pathways during the treatment of methyl tert-butyl ether by the UV/H2O2 process. Environ. Sci. Technol, v. 34, pp. 650-658, 2001.

[18] Vicente, R., Rodolfo Z., Gloria D., Ricardo, G.: MTBE visible-light photocatalytic decomposition over Au/TiO2 and Au/TiO2–Al2O3 sol–gel prepared catalysts, Journal of Molecular Catalysis A: Chemical, Volume 281, Issues 1-2, 18 February 2008.

[19] Melnick, R., Kohn, M., and Portier, C.: Implications for risk assessment, 1996.

[20] Mezyk, S., Cooper, W., Bartels, D., O'Shea, K. and Wu, T.: Radiation chemistry of alternative fuel oxygenates: substituted ethers. J. Phys. Chem.Part A, v. 105, pp. 3521-3526 (2001).

[21] Mitani, M., Keller, A., Golden, S. and Hatfield, R., Cheetham, A.: Low temperature catalytic decomposition and oxidation of MTBE, Applied Catalysis B: Environmental, Volume 34, Issue 2, 5 November 2001.

[22] Malcolm, P.: Taste and Odor Properties of Methyl Tertiary-Butyl Ether and Implications for Setting a Secondary Maximum Contaminant Level. Prepared for the Oxygenated Fuels Association, Inc., June 1998.

[23] Michael, M., Janshekar, M.: Gasoline Octane improve/Oxygenates. SRI C SRIConsulting.http://www.sriconsulting.com/CEH/Public/Reports/543.7500. Published April 2006

[24] Moran, M., Zogorski, J. and Squillace, P.: MTBE in groundwater of the united states- occurrence, potential sources and long-range transport, AWWA Water Resources Conference, Norfolk, Virginia, 1999.

[25] National Science and Technology Council (NSTC). Interagency assessment of IC., 1996.

[26] Qinhai, H., Chunlong, Z., Zhirong, W., Yan C., Kehui, M., Xingqing Z., Yunlong, X. and Miaojun, Z.: Photodegradation of methyl tert-butyl ether (MTBE) by UV/H_2O_2 and UV/TiO_2, Journal of Hazardous Materials, Volume 154, Issues 1-3, pages 795-803, 2008.

[27] Raese, J., Rose, D. and Sandstrom, M.: U.S. Geological survey laboratory method for Methyl Tert-Butyl Ether and other fuel oxygenates. In Fact Sheet 219-95; U.S. Geological Survey, p. 4., 1995.

[28] Sang Eun, P., Hyunku, J., JoonWun, K.: Photodegradation of methyl tertiary butyl ether (MTBE) vapor with immobilized titanium dioxide, Solar Energy Materials and Solar Cells, Volume 80, Issue 1, 15 October 2003.

[29] Sergei, P., Anna, K., NuriaCapdet, S.: The dependence on temperature of gas-phase photocatalytic oxidation of methyl tert-butyl ether and tert-butyl alcohol, Catalysis Today, Volume 101, Issues 3-4, 15 April 2005.

[30] Stocking, A., Suffet, I., McGuire, M. and Kavanaugh, M.: Implications of an MTBE odor study for setting drinking water standards. Jour. AWWA, v.93,, 2001.

[31] Squillace, P., Pankow, J., Korte, N. and Zogorski, J.: Review of the behavior and fate of Methyl Tert-Butyl Ether. Environmental Toxicology and Chemistry, v. 16, 1997.

[32] USEPA. Achieving Clean Air and Clean Water: The Report of Blue Ribbon Panel on Oxygenates in Gasoline. EPA 420-R-99-021., 1999.

[33] USEPA. MTBE Fact Sheet #3, Use and Distribution of MTBE and Ethanol. EPA 510-F97-016. Office of Solid Waste and Emergency Response. Washington, D.C., 1998.

[34] www.shellchemicals.com

[35] www.waterquality.crc.org.au)

[36] http://en.wikipedia.org/wiki/Gas_chromatography#Physical_components

[37] http://en.wikipedia.org/wiki/Solid_phase_microextraction

[38] Chung, F.: "Quantitative Interpretation of X-ray Diffraction Patterns of Mixtures III. Simultaneous Determination of a Set of Reference Intensities," Journal of Applied Crystallography, Vol. **8,** 1975.

[39] Klug, H. and Alexander, L.: X-ray Diffraction Procedures for Polycrystalline and Amorphous Materials, 2nd ed., New York: John Wiley, 1974.

[40] O'Connor, B., Li, D. and Sitepu, H.: "Strategies for Preferred Orientation Corrections in X-ray Powder Diffraction Using Line Intensity Ratios," Advances in X-ray Analysis, Vol. 34, 1999.

[41] Sitepu, H., O'Connor, B. and Li, D.: "Comparative Evaluation of the March and Generalized Spherical Harmonic Preferred Orientation Models Using X-ray Diffraction Data for Molybdite and Calcite Powders," Journal of Applied Crystallography, Vol. 38, No.1, March 2005.

[42] Sitepu, H.: "Use of the Rietveld Method for Describing Structure and Texture in XRD Data of Dolomite [CaMg(CO3)2] and Hydromagnesite [Mg5(CO3)4(OH)2(H2O)4] Powders," Advances in X-ray Analysis, Vol. 55, 2012.

[43] Shama, R.: Strategies of making TiO_2 and ZnO visible light active Journal of Hazardous Materials, Volume 170, Issues 2–3, 30 October 2009.

[44] Wu, Y., Xing, M., Zhang, J., and Chen, F.: Effective visible light-active boron and carbon modified TiO_2 photocatalyst for degradation of organic pollutant. Applied Catalysis B: Environmental, Volume 97, Issues 1–2, 9 June 2010.

[45] Wan-Kuen, J., Chang-Hee, Y.: Visible-light-induced photocatalysis of low-level methyl-tertiary butyl ether: Department of Environmental Engineering, Kyungpook National University, Sankeokdong, Bukgu, Daegu 702-701, South Korea, 2009.

[46] http://en.wikipedia.org/wiki/Gas_chromatography%E2%80%93mass_spectrometr

VITAE

Name:	Saleh H. Al-Sharidi
Nationality:	Saudi Arabian
Mail Address:	P.O. Box 1916 , Dhahran 31311 Saudi Arabia
Home Address:	Al-Khobar North, Saudi Arabia
Contacts:	Mobile: 0555812968 E-mail: shardham4@yahoo.com

Education/Training:

Education:	B. S. Degree in Chemistry, University of Arizona, Tucson, Arizona. (August 1991).

Career History:

April 1992	Joined the Saudi Aramco Research and Development Center
1992-1997	Geochemistry unit working on the Specialty of Isotope Ration Mass Spectrometer (IRMS).
2000-2004	Environmental Unit as solid waste group leader and acting supervisor during the period of August 15 to September 15, 2004.
2005-2007	Environmental unit supervisor
2008-2010	Supervisor for Chemistry Analysis Unit, R&DC Environmental Coordinator, R&DC Management representative on implementing ISO14001 Environmental management System for R&DC
2013	Supervisor for Process Support Unit